AD-A-248430

REPORT DOCUMENTATION PAGE

Form Approved
OMB No. 0704-0188

1. AGENCY USE ONLY (Leave blank)	2. REPORT DATE	3. REPORT TYPE AND DATES COVERED
	January 1, 1992	Final 11-1-88 through 10-31-91

4. TITLE AND SUBTITLE

Millimeter-Wave Grid Oscillators

5. FUNDING NUMBERS

DAAL03-89-K-0003

6. AUTHOR(S)

David Rutledge

7. PERFORMING ORGANIZATION NAME(S) AND ADDRESS(ES)

Caltech, Pasadena, CA 91125

8. PERFORMING ORGANIZATION REPORT NUMBER

9. SPONSORING/MONITORING AGENCY NAME(S) AND ADDRESS(ES)

U. S. Army Research Office
P. O. Box 12211
Research Triangle Park, NC 27709-2211

10. SPONSORING/MONITORING AGENCY REPORT NUMBER

ARO 26381.18-EL

11. SUPPLEMENTARY NOTES

The view, opinions and/or findings contained in this report are those of the author(s) and should not be construed as an official Department of the Army position, policy, or decision, unless so designated by other documentation.

12a. DISTRIBUTION/AVAILABILITY STATEMENT

Approved for public release; distribution unlimited.

12b. DISTRIBUTION CODE

13. ABSTRACT (Maximum 200 words)

Active grids dramatically increase the power-handling ability of solid-state devices by quasi-optical power combining. We report progress in three areas—oscillator grids, mixer grids, and amplifier grids. Several different grids with up to 100 devices have been demonstrated and accurate circuit models have been developed. This work should make high-power millimeter-wave monolithic circuits for radars and communications systems possible.

14. SUBJECT TERMS

Millimeter-wave systems, grid oscillators, grid mixers, grid amplifiers.

15. NUMBER OF PAGES

16. PRICE CODE

17. SECURITY CLASSIFICATION OF REPORT	18. SECURITY CLASSIFICATION OF THIS PAGE	19. SECURITY CLASSIFICATION OF ABSTRACT	20. LIMITATION OF ABSTRACT
UNCLASSIFIED	UNCLASSIFIED	UNCLASSIFIED	UL

Final Report
Millimeter-Wave Grid Oscillators

David Rutledge
California Institute of Technology
January 1, 1992
U.S. Army Research Office
Contract DAAL03-89-K-0003

The Problem—Quasi-optical power combining

The maximum output powers of microwave and millimeter-wave solid-state devices are quite small compared to vacuum tubes, and this limits the application of solid-state devices in many radar and communications systems. This suggests that we consider combining the outputs of a large number of solid-state devices. Following James Mink's proposal of quasi-optical power combining as a way to overcome the limits imposed by waveguide and transmission-line power combiners [1], Young and Stephan showed that microstrip patch oscillators can be combined in a quasi-optical resonator by inter-injection locking [2]. Then Popović *et al.* demonstrated large-scale power combining with inter-injection locking in a 25-MESFET oscillator grid [3]. In addition, a monolithic millimeter-wave phase-shifter grid [4] and multiplier [5] were fabricated. In each of these devices, the total power scales as the grid area, but the embedding impedances are determined by the dimensions of the unit cell. This allows a designer to optimize the unit cell to achieve maximum efficiency and minimum noise, and to independently choose the area to meet the power requirement. These initial results were promising, but there were several serious problems. The oscillator grids were designed empirically, and the number of transistors was rather limited. In addition, the bias connections required holes punched through the circuit board, making them difficult to fabricate as a monolithic circuit. No provisions were made for getting rid of excess heat. In addition, other basic grid components—amplifiers and mixers, were missing.

Results—Oscillator, mixer, and amplifier grids

We have results in three areas—oscillators, mixers and amplifiers. Details are given in the copies of recent papers that are attached as an Appendix. The oscillator grids are most developed; amplifier and mixer work is just beginning.

In two papers by Popović *et al.* [6,7] we made several advances. A grid was made on brass bars, which served as a heat sink. The effect of the bars on the circuit was taken into account in the analysis. Next a 100-MESFET grid oscillator was demonstrated. Even though the total output power was only half a watt, it showed that a large number of devices could be locked together. In addition, a circuit model was developed that predicted the embedding impedances accurately. This circuit was also planar, and would be suitable for fabrication as a monolithic integrated circuit in the millimeter-wave range. More recently Weikle *et al.* demonstrated a grid circuit using gate feedback to sustain the oscillation [Appendix A]. This circuit gave more than twice as much power per transistor at more than twice the frequency of the previous circuit. We believe the gate-feedback grid will be the basis for future high-power designs.

Jon Hacker developed a Schottky-diode mixer grid with 100 diodes that is suitable for mixing quasi-optical beams [Appendix B]. He showed that the dynamic range

of the mixer was increased by 20 dB over that of a single diode mixer. The circuit can be made as a planar hybrid circuit or a monolithic circuit, no metal waveguide is required. We feel that the main application of these grids is at very high frequencies in the submillimeter band where superconductor-insulator-superconductor (SIS) mixer suffer from severe overloading problems, and metal waveguides become difficult to fabricate.

The most critical element that would be needed to develop high-power solid-state systems with grids is an amplifier. After several failures in previous years, Moonil Kim finally succeeded last spring [Appendix C]. He built a 50-MESFET grid with a gain of 11 dB at 3.3 GHz. The unit cell in the grid is a pair of MESFET's with their sources tied together to act as a differential amplifier. The fifty MESFET's are arranged as 25 differential amplifiers that accept a vertically polarized input and transmit a horizontally polarized output. A simple calibration procedure allows the gain to be calculated from a relative power measurement. The design should be suitable for monolithic wafer-scale integration, particularly at millimeter wavelengths.

In the future, we hope to shift to designing monolithic millimeter-wave grids for fabrication by industry. We have developed relations with the Martin-Marietta Corporation, for grids with high-electron mobility transistors (HEMT's), the Rockwell Science Center, for fabrication of grids, with heterojunction bipolar transistors (HBT's), and the Jet Propulsion laboratory, for fabrication of HEMT and SIS grids. Martin-Marietta and Rockwell have already made oscillator grids designed for the 40 to 90 GHz range, and we are now testing them. All three laboratories have indicated a strong interest in building grid amplifiers. In addition, a major goal will be to demonstrate high power, in the 50-Watt range, from a hybrid circuit, and to build low-noise circuits.

Grid amplifiers offer exciting possibilities. A grid amplifier is a multi-mode device, and should amplify beams at different angles. For example, it should be possible to place a grid amplifier after an electronic beam-steering array. The grid would amplify both single and multiple transmitted beams, while preserving propagation angles, sidelobe levels, and monopulse nulls. The amplifier could overcome losses in the beam steerer itself. A grid amplifier could also precede a receiving beam-steering array, allowing the noise performance to be determined by the grid, rather than by losses in the beam steerer.

Conferences and Papers

1. "Frontiers in Antenna Applications," David Rutledge, Invited plenary talk, International Symposium, San Jose, CA, June 1989.

2. "Quasi-optical Watt-Level Millimeter-Wave Monolithic Solid-State Diode-Grid Frequency Multipliers," R. J. Hwu, L. P. Sadwick, N. C. Luhmann, D. B. Rutledge, M. Sokolich, B. Hancock, International Microwave Symposium, Long Beach, CA, June, 1989.

3. "Advances in monolithic horn-antenna imaging arrays," P. Stimson, Yong Guo, Karen Lee, and D. Rutledge, 13th Annual Antenna Applications Symposium," Robert Allerton Park, IL, September, 1989.

4. "Multi-element quasi-optical devices—a new trend in millimeter and submillimeter-wave electron devices," Koji Mizuno and David Rutledge, 14th International Conference on Infrared and Millimeter Waves, Wurzburg, Germany, October 1989.

5. "Perspectives in Microwave Circuit Analysis," R. C. Compton and D. B. Rutledge, Symposium on Circuits and Systems, Urbana, IL August 1989.

6. "Microwave and Millimeter-Wave Frequency Multiplier Arrays," R. J. Hwu, N. C. Luhmann, Jr., D. B. Rutledge, B. Hancock, and U. Lieneweg, 14th International Conference on Infrared and Millimeter Waves, Wurzburg, Germany, October 1989.

7. "Monolithic Integration of Varactor Diodes on III-V Compound Semiconductors for Watt-Level Frequency Multiplication in the Millimeter-Wave Region," R. J. Hwu, L. P. Sadwick, N. C. Luhmann, Jr., D. B. Rutledge, and M. Sokolich, Second International Conference on Solid-State and Integrated-Circuit Technology, Beijing, China, October 22–28, 1989.

8. "Aperture Efficiency of Chemically Etched Horns at 93 GHz," Yong Guo, Karen Lee, Philip Stimson, Kent A. Potter, and David B. Rutledge, submitted to the International Antenna and Propagation Symposium, Dallas, Texas, May, 1990.

9. "Large Area Bolometers for Millimeter-Wave Power Calibration," Gabriel M. Rebeiz, Curtis C. Ling, and David B. Rutledge, *Int. J. Infrared and Millimeter Waves, 10*, pp. 931–936, 1989.

10. "Array Concepts for Solid-State and Vacuum Microelectronics Millimeter-Wave Generation," R. J. Hwu, N. C. Luhmann, Jr., W. W. Lam, Z. B. Popović, and D. B. Rutledge, *IEEE Trans. on Electron Devices, ED-36*, pp. 2645–2650, 1989.

11. "Bar-Grid Oscillators," Z. B. Popović, R. M. Weikle, M. Kim, K. A. Potter, and D. B. Rutledge, *IEEE Trans. on Microwave Theory and Techniques, MTT-38*, pp. 225–230, 1990.

12. "Quasi-Optical Power-Combining Arrays," D. B. Rutledge, Zoya Basta Popović, Robert M. Weikle, II, Moonil Kim, Kent A. Potter, Richard C. Compton, and Robert A. York, International Microwave Theory and Techniques Symposium, Dallas Texas, May, 1990.

13. "A 100-Element MESFET Grid Oscillator," Robert M. Weikle, II, Zoya Basta Popović, Moonil Kim, Kent A. Potter, and D. B. Rutledge, International Antenna and Propagation Symposium, Dallas, Texas, May, 1990.

14. "Aperture Efficiency of Chemically Etched Horns at 93 GHz," Yong Guo, Karen Lee, Philip Stimson, Kent A. Potter, and David B. Rutledge, International Antenna and Propagation Symposium, Dallas, Texas, May, 1990.

15. "Grid Oscillators," Ph.D. Thesis by Zorana Popović, California Institute of Technology, June, 1990.

16. "Technology for Millimeter-Wave Imaging," David Rutledge, Yagi Symposium, 2nd Annual Sendai Conference, Sendai, Japan, September, 1990.

17. "Adjustable RF Tuning Elements for Planar Millimeter Wave and Submillimeter Wave Circuits," W.R. McGrath, V. Lubecke, and David Rutledge, 15th International Conference on Infrared and Millimeter Waves, Orlando, Florida, December, 1990.

18. "S Parameter measurements of Quantum-Well Devices," Olga Borić, Timo J. Tolmunen, Maragaret A. Frerking, Jonathan B. Hacker, and David B. Rutledge, 15th International Conference on Infrared and Millimeter Waves, Orlando, Florida, December, 1990.

19. "Progress in Grid Oscillators," Zoya Basta Popović, Robert M. Weikle, II, Moonil Kim, David B. Rutledge, 15th International Conference on Infrared and Millimeter Waves, Orlando, Florida, December, 1990.

20. "Development of a monolithic 94 GHz quasi-optical 360 degree phase shifter," L. B. Skogren, R. J. Hwu, W. Wu, X.-H. Qin, N. C. Luhmann, Jr., M. Kim, and D. B. Rutledge, 15th International Conference on Infrared and Millimeter Waves, Orlando, Florida, December, 1990.

21. "Modeling of Tunable Planar Circuits for Millimeter and Submillimeter Wave Applications," V. M. Lubecke, W. R. McGrath, and D. B. Rutledge, 2nd International Symposium on Space Terahertz Technology, February 1991.

22. "Monolithic millimeter-wave two-dimensional horn imaging arrays," G. M. Rebeiz, D. P. Kasilingam, Y. Guo, and P. A. Stimson, and D. B. Rutledge, *IEEE Trans. on Antennas and Propagat. AP9*, pp. 1473–1482, 1990.

23. "A 100-Element Schottky Diode Grid Mixer," Jonathan B. Hacker, Robert M. Weikle, II, Moonil Kim, and David B. Rutledge, IEEE Antenna and Propagation Society Symposium, London, Ontario, June 1991.

24. "An X-Band MESFET Grid Oscillator with Gate Feedback," Robert M. Weikle, II, Moonil Kim, Jonathan B. Hacker, and David B. Rutledge, IEEE Antenna and Propagation Society Symposium, London, Ontario, June 1991.

25. "A 100-MESFET Planar Grid Oscillator," Z. B. Popović, R. M. Weikle, II, M. Kim, and D. B. Rutledge, *IEEE Transactions on Microwave Theory and Techniques, MTT-39*, pp. 193–200, 1991.

26. "Aperture Efficiency of Integrated-Circuit Horn Antennas," Yong Guo, Karen Lee, Philip Stimson, Kent Potter, and David Rutledge, *Microwave and Optical Technology Letters*, 4, pp. 6–9, 1991.

27. "Thin-Film Power-Density Meter for Millimeter Wavelengths," K. Lee, Y. Guo, P. Stimson, K. Potter, and D. Rutledge, *IEEE Transactions on Antennas and Propagation, AP-39,* pp. 425–428, 1991.

28. "A Grid Amplifier," Moonil Kim, James J. Rosenberg, R. Peter Smith, Robert M. Weikle, II, Jonathan B. Hacker, Michael P. DeLisio, and David B. Rutledge, *IEEE Microwave and Guided Wave Letters, 1,* Nov. 1991, pp. 322–324.

29. "A 100-Element Planar Schottky Diode Grid Mixer," Jonathan B. Hacker, Robert M. Weikle, II, Moonil Kim, Michael P. DeLisio, and David B. Rutledge, to be published in *IEEE Transactions on Microwave Theory and Techniques.*

30. "Planar MESFET grid oscillators using gate feedback," Robert M. Weikle, II, Moonil Kim, Jonathan B. Hacker, Michael P. DiLisio, and David B. Rutledge, submitted to *IEEE Trans. on Microwave Theory and Tech.*

31. "Quasi-Optical Receiver Technology," David B. Rutledge, Robert M. Weikle, Moonil Kim, Jonathan B. Hacker, and Michael P. DeLisio, 16th International Conference on Infrared and Millimeter Waves, Lausanne, Switzerland, August 1991.

32. "Transistor Oscillator and Amplifier Grids," Robert M. Weikle, Moonil Kim, Jonathan B. Hacker, Michael P. DeLisio, Zoya Popović, and David B. Rutledge, submitted to *Proceedings of the IEEE.*

33. "Quasi-Optical Planar Grids for Microwave and Millimeter-Wave Power Combining," Robert M. Weikle, II, Ph.D. Thesis, California Institute of Technology, 1991.

Scientific Personnel

This contract has supported six Ph.D students:

Zorana Popović developed the original oscillator grids. She is now an assistant professor at the University of Colorado at Boulder.

Bobby Weikle developed the idea of oscillator grids with gate feedback in his Ph.D. thesis work. He has now gone to Chalmers University in Sweden. He has a postdoctoral fellowship under Erik Kollberg, and plans to build monolithic oscillator grids.

Moonil Kim is a fourth-year graduate student. He has been developing grid amplifiers. He has been testing a grid amplifier that uses 200 HEMT's. This grid is designed to operate at 10 GHz. In addition, he is testing an amplifier grid with differential amplifier chips that were specially made by the Rockwell Science Center. These chips have two heterojunction bipolar transistors with their emitters connected as a long-tail pair. He is also testing monolithic oscillator grids from Rockwell. These grids use HBT's, and are designed to operate at 44 GHz.

Jon Hacker is a fourth-year graduate student. He developed the Schottky-diode mixer grid, and is currently working on a high-power oscillator grid that he hopes will produce 50 watts at 10 GHz.

Michael DiLisio is a second-year graduate student. He is testing monolithic oscillator grids from Martin Marietta. The Martin-Marietta grids use HEMT's, and are designed to operate at 94 GHz.

Shijie Li is a first-year graduate student. She is building a one-dimensional line oscillator, which are intended as the building blocks for steerable two-dimensional arrays.

PATENTS

We are filing for a patent on the grid amplifier.

BIBLIOGRAPHY

[1] James W. Mink, "Quasi-optical Power Combining of Solid-State Millimeter-Wave Sources," *IEEE Trans. on Microwave Theory and Tech.*, *MTT-34*, pp. 273–279, 1986.

[2] S. Young and K. D. Stephan, "Stabilization and Power Combining of Planar Microwave Oscillators with an Open Resonator," *IEEE International Microwave Symposium Digest*, pp. 185–188, 1987.

[3] Z. B. Popović, M. Kim, and D. B. Rutledge, "Grid Oscillators," *Int. J. Infrared and Millimeter Waves, 9*, pp. 647–654, 1988.

[4] W. W. Lam *et al.*, "Millimeter-wave diode-grid phase shifters," *IEEE Trans. Microwave Theory Tech.*, *MTT36*, pp. 902–907, 1988.

[5] C. F. Jou *et al.*, "Millimeter-wave diode-grid frequency doubler," *IEEE Trans. Microwave Theory Tech., MTT36*, pp. 1507–1514, 1988.

[6] Z. B. Popović, R. M. Weikle, M. Kim, K. A. Potter, and D. B. Rutledge, "Bar-Grid Oscillators," *IEEE Trans. on Microwave Theory and Techniques*, *MTT-38*, pp. 225–230, 1990.

[7] Z. B. Popović, R. M. Weikle II, M. Kim, and D. B. Rutledge, "A 100-MESFET Planar Grid Oscillator," *IEEE Trans. on Microwave Theory and Tech.*, *MTT-39*, pp. 193–200, 1991. A reprint is included in the appendix.

APPENDICES—REPRINTS

[A] "Planar MESFET grid oscillators using gate feedback," Robert M. Weikle, II, Moonil Kim, Jonathan B. Hacker, Michael P. DiLisio, and David B. Rutledge, submitted to *IEEE Trans. on Microwave Theory and Tech.*

[B] "A 100-Element Planar Schottky Diode Grid Mixer," Jonathan B. Hacker, Robert M. Weikle, II, Moonil Kim, Michael P. DeLisio, and David B. Rutledge, to be published in *IEEE Transactions on Microwave Theory and Techniques.*

[C] "A Grid Amplifier," Moonil Kim, James J. Rosenberg, R. Peter Smith, Robert M. Weikle, II, Jonathan B. Hacker, Michael P. DeLisio, and David B. Rutledge, *IEEE Microwave and Guided Wave Letters, 1*, Nov. 1991, pp. 322–324.

Submitted to the *IEEE Transactions on Microwave Theory and Techniques*, August 1991

Planar MESFET Grid Oscillators using Gate Feedback

Robert M. Weikle, II, Moonil Kim, Jonathan B. Hacker
Michael P. De Lisio, David B. Rutledge

Division of Engineering and Applied Science
California Institute of Technology
Pasadena, CA 91125

Abstract— **A new method for quasi-optically combining the output power of MESFET's is presented in which drain and source leads couple directly to the radiated field. The design consists of a planar grid of devices placed in a Fabry-Perot cavity. Capacitive feedback is provided to the gate. This is in contrast to previous MESFET grid designs where the radiated electric field was coupled to the drain and gate currents [12]. The new gate-feedback grids can oscillate at much higher frequencies than these previous grids. The oscillation frequency is dependent on the device characteristics, the resonator cavity, and is also a function of the symmetries of the grid. A transmission-line model for the grid is discussed and used to design two oscillator arrays. Experimental results are presented for oscillator grids operating at X-band and Ku-band. A 16-element grid has produced 335 mW of power at 11.6 GHz with a DC-to-RF conversion efficiency of 20%. This design was scaled to produce a 36-element grid ocillator with output power of 235 mW at 17 GHz. These results represent a significant improvement in the performance of planar grid oscillators which were previously limited to an operating frequency of 5 GHz and output power of 6 mW per device when using the same transistor. In addition, the planar configuration of the grid is very convenient for monolithic integration and is easily scalable to millimeter-wave frequencies.**

I. Introduction

In recent years, power-combining schemes involving microwave and millimeter-wave solid-state sources have received much attention. The development of high-power, efficient and reliable sources is necessary to take advantage of the broader bandwidths and higher resolution imaging possible at millimeter-wave frequencies. High-power vacuum tubes are capable of producing better than 100 W at 100 GHz but the size, weight, and required high-voltage power supplies often limit their usefulness [1]. Solid-state technology can provide devices that operate in the millimeter-wave range, however, the

power output from these devices is quite limited. IMPATT's can produce a few watts of CW power at 100 GHz while Gunn diodes are capable of producing about 100 mW. In addition, Gunn diodes and IMPATT's suffer from poor DC-to-RF efficiencies [2]. Better efficiencies can be realized with transistors. Pseudomorphic HEMT amplifiers have produced output powers of 57 mW at 94 GHz and power-added efficiencies of over 20% [3]. Heterojunction bipolar transistors also have the potential to provide high power at millimeter-wave frequencies without need for sub-micron lithography. An HBT with emitter area of 80 μm^2 has shown 15 dB of gain with an output power of 16 dBm at 35 GHz [4].

A variety of methods for combining the output powers of solid-state devices have been developed. A good review of these methods is given by Russell [5] for the microwave region and Chang and Sun for millimeter-wave frequencies [6]. Many of these techniques involve resonant microwave cavities or hybrids that are scaled for millimeter-wave operation. There are several disadvantages to this approach. The size of the cavities must be scaled according to wavelength making ciruit fabrication more difficult. Waveguide losses also become more severe at millimeter-wave frequencies. In addition, a power-combiner based on resonant cavities or hybrid couplers can only accomodate a limited number of devices.

An attractive approach for overcoming the limitations of conventional waveguide and hybrid power-combiners is to combine the output powers of many devices in free-space. Mink suggested using an array of millimeter-wave devices placed in an optical resonator as a means of large-scale power-combining [7]. Because the power is combined in free-space, losses associated with waveguide walls and feed networks are eliminated. The power can be distributed over a large number of devices which is advantageous for high-power applications. In addition, synchronization or locking of the devices is accomplished with optical resonators which are easily realizable at millimeter-wave frequencies.

Several types of quasi-optical power-combiners have been reported in the literature. One design utilizes an array of packaged devices placed on a grid of metal bars [8], [9]. The metal bars provide an excellent heat sink which is necessary for low efficiency devices such as Gunn diodes. Another approach involves an array of weakly coupled patch antenna elements [10]. This method is similar to classic antenna arrays in which each individual patch is a free-running oscillator containing an active device. The patch elements are synchronized through the use of a partially transmitting reflector placed above the array. More recently, a two-sided microstrip configuration has been developed which permits isolation between an injection-locking signal and the array output [11]. A different design using a planar grid containing 100 packaged MESFET's in which all the devices lie in the same plane was developed by Popović, *et al.* [12]. This grid produced an output power of 600 mW at 5 GHz with a DC-to-RF efficiency of 20%. The approach relies on the symmetries of the grid to provide the impedances necessary for oscillation to occur. The structure is most similar to a laser oscillator in which the grid of MESFET's acts as a gain medium inside a Fabry-Perot cavity.

An advantage of the planar configuration is its amenability to wafer-scale integration, wbich is necessary for scaling to millimeter-wave frequencies.

In this paper, we introduce a new planar grid configuration. The design permits higher frequency operation than possible with previous planar grid configurations. A simple transmission-line model is used for the design. Results for oscillator grids operating in the X-band and Ku-band are presented.

II. Grid Configuration

There are two important factors which determine the behavior of a quasi-optical array. The first is the cboice of devices used in tbe grid. Gunn diodes and IMPATT's have the advantage of being two-terminal devices and are thus easily incorporated into a grid array. The low DC-to-RF efficiency, however, is a major drawback. In addition, Gunn diodes are inherently unstable and synchronization can prove difficult. Others have found it necessary to individually bias eacb device in the array to facilitate locking [10]. In contrast, transistors have a control terminal which is separate from the output terminals. This permits the devices in the grid to be more easily stabilized, allowing tbe oscillation to be controlled througb an appropriately designed feedback network.

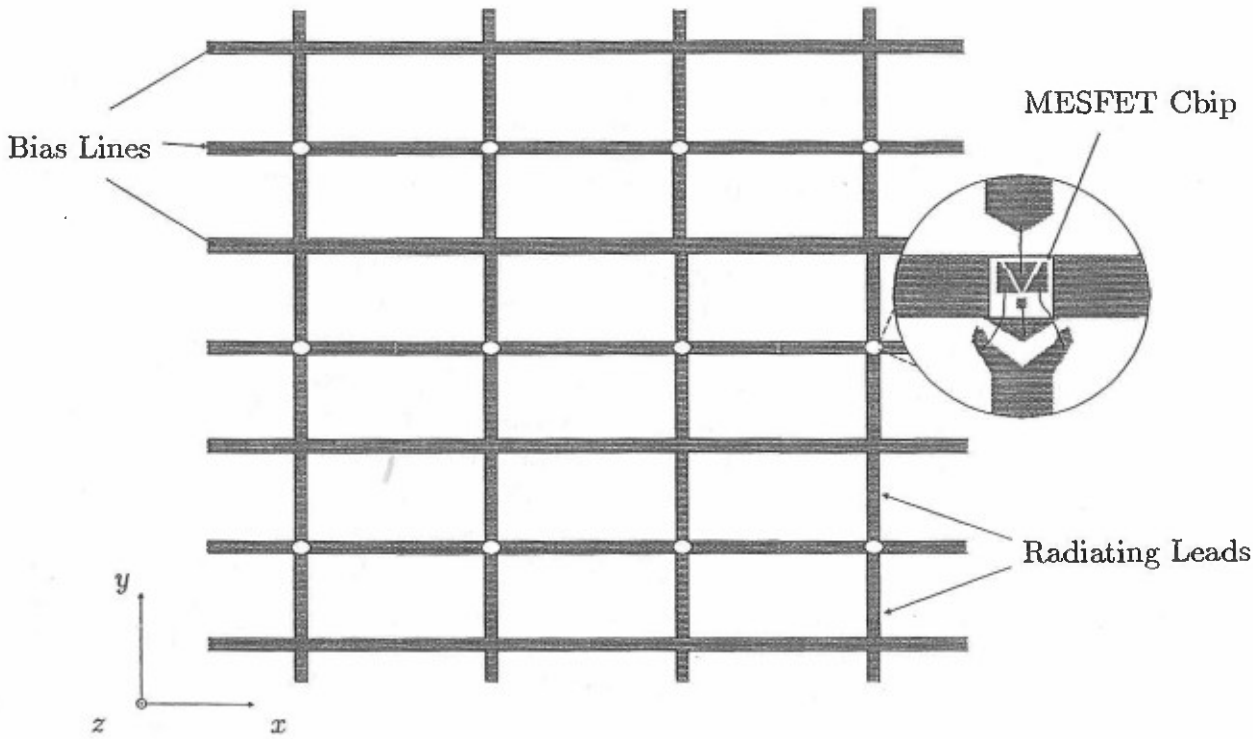

Figure 1. Physical layout of the planar MESFET grid. MESFET's are represented as open circles and are placed at each node of the grid. Adjacent rows of devices share bias lines. The inset shows the detail of a transistor chip wire-bonded to the grid.

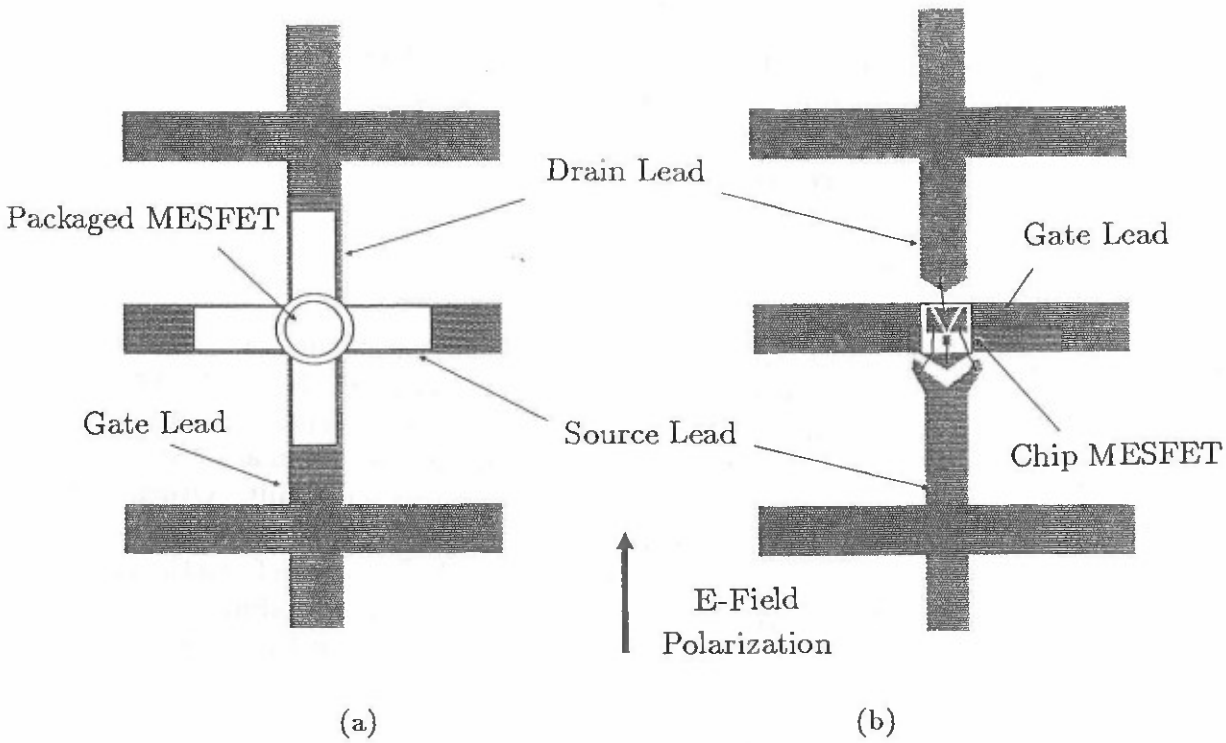

Figure 2. (a) Unit cell for previous grid oscillators with packaged MESFET's. The drain and gate leads are parallel to the incident electric field. (b) Unit cell for the gate-feedback grid oscillator with chip MESFET's. The drain and source couple directly to the incident electric field. The gate leads, which run horizontally, are capacitively coupled to the incident field.

The second major factor determining the behavior of a quasi-optical array is the grid's physical configuration. The grid structure, together with the optical resonator, provides an embedding circuit in which the solid-state devices are placed. The oscillation frequency, output power, and efficiency of the grid depend on the impedances this embedding circuit presents at the device terminals. The planar MESFET grid configuration is shown in Fig. 1. The MESFET's are placed at each node in the grid and are represented by open circles. The details of how the transistor is connected to the grid depends on the physical layout of the device and several options are possible. The DC bias is fed along horizontal leads which extend across the grid in the x-direction. Adjacent rows of devices share bias lines. The radiating leads run in the y-direction and are connected to two terminals of the transistor. The third MESFET terminal is connected to the center bias line which runs along the row of devices.

Previous work with planar MESFET grids utilized packaged devices [12]. One cell of this grid is shown in Fig. 2(a). The use of packaged devices (Fujitsu FSC11LF) restricted the grid to a vertical drain-gate configuration. The disadvantage of this design is that the gate lead of the transistor radiates. As a result, the MESFET gate

is always strongly coupled to the radiated field and this leads to oscillation at lower frequencies where the devices have high gain.

A configuration which overcomes this problem is shown in Fig. 2(b). Using a chip transistor the restrictions imposed by the package are eliminated and a vertical drain-source configuration can be realized. Bond wires are used to connect the device leads to the grid. The MESFET gate lead runs perpendicular to the radiated field and the feedback between the radiated field and gate now occurs through the MESFET embedding circuit.

III. Transmission-Line Model

To understand the behavior of a quasi-optical grid oscillator, it is necessary to know what impedances are present at the terminals of a MESFET placed in the array. The grid transmission-line model is based on an assumption that all devices in the grid are identical. For a grid infinite in extent, each transistor lies in an equivalent unit cell which is defined by the grid symmetry. The field radiated by the infinite grid must satisfy symmetry-imposed boundary conditions at the unit cell edges as shown in Fig. 3. The unit cell is thus an equivalent waveguide representation for the entire grid. This equivalent waveguide has electric walls on the top and bottom and magnetic walls on the sides. It extends in the $+z$ and $-z$ directions, with the MESFET in the $z = 0$

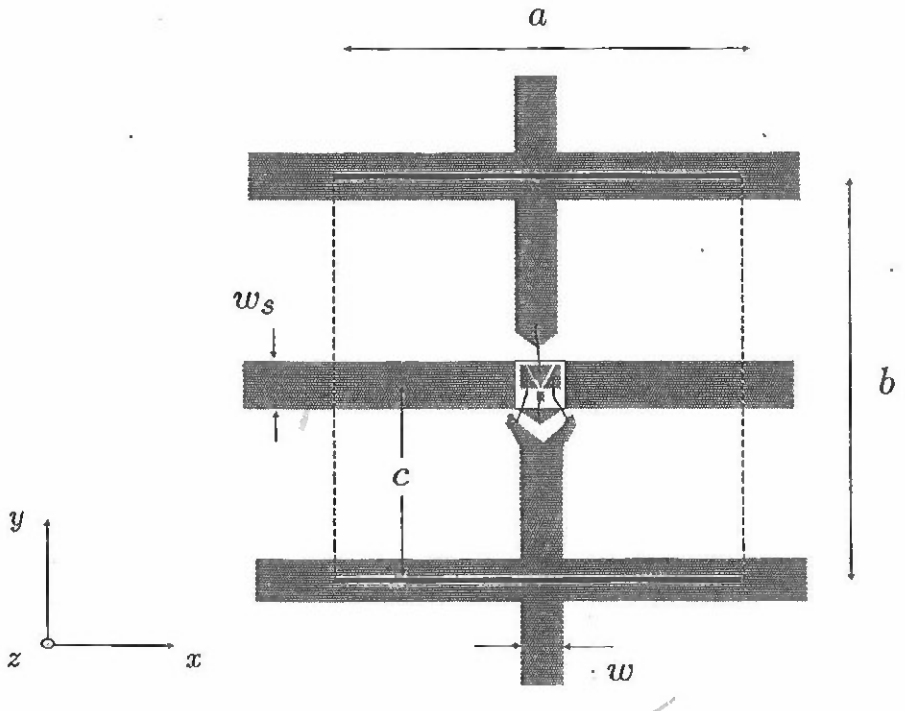

Figure 3. Definition of the unit cell equivalent waveguide. The unit cell dimensions are indicated by the variables on the diagram. Electric walls are represented with solid lines and magnetic walls are represented with dashed lines.

plane. A transmission-line model representing the unit cell can be obtained using an EMF analysis similar to that of Eisenhart and Khan for a post in a waveguide [13]. The details of this analysis have been given elsewhere and it is not necessary to repeat them here [12].

The transmission-line model for the grid is shown in Fig. 4(a). The terminals labeled 1 and 2 represent connections to the vertical leads of the grid. The center terminal labeled 3 represents the horizontal lead. Currents in the vertical leads couple to the radiated field through a center-tapped transformer. Free space is modeled with a $377\,\Omega$ resistor which is scaled by the aspect ratio (b/a) of the unit cell. The mirror behind the grid is represented with a shunt short-circuited stub. The inductance of the radiating leads is shown as a series lumped inductor L. The horizontal leads do not couple directly to the radiated field but do produce evanescent modes which are modeled with a series capacitor and inductor (C_m and L_m). Expressions for the elements in the equivalent circuit model are derived from the EMF analysis and are given by :

$$L = \frac{2b}{j\omega a} \sum_{\substack{m>0 \\ m \text{ even}}}^{\infty} \operatorname{sinc}^2\left(\frac{m\pi w}{2a}\right) Z_{m0}^{TE} \tag{1}$$

$$L_m = \frac{4}{j\omega ab} \sum_{\substack{m \text{ even} \\ m,n\neq 0}}^{\infty} \frac{1}{k_c^2} \sin^2\left(\frac{n\pi c}{b}\right) \operatorname{sinc}^2\left(\frac{m\pi w}{2a}\right) \operatorname{sinc}^2\left(\frac{n\pi w_s}{2b}\right) \times \tag{2}$$

$$\left(\frac{k_x}{k_y} + \frac{k_y a}{k_x(a-w)}\right)^2 Z_{mn}^{TE}$$

$$\frac{1}{C_m} = j\,\frac{2\omega}{ab}\left(\sum_{n=1}^{\infty} \frac{1}{k_y^2} \sin^2\left(\frac{n\pi c}{b}\right) \operatorname{sinc}^2\left(\frac{n\pi w_s}{2b}\right) Z_{0n}^{TM} + \right. \tag{3}$$

$$\left. 2\sum_{\substack{m \text{ even} \\ m,n\neq 0}}^{\infty} \frac{1}{k_c^2} \sin^2\left(\frac{n\pi c}{b}\right) \operatorname{sinc}^2\left(\frac{n\pi w_s}{2b}\right) \operatorname{sinc}^2\left(\frac{m\pi w}{2a}\right) \left(1 - \frac{a}{a-w}\right)^2 Z_{mn}^{TM} \right)$$

In the above expressions $k_x = m\pi/a$, $k_y = n\pi/b$, and $k_c^2 = k_x^2 + k_y^2$, where m and n are integers. Z_{mn}^{TE} and Z_{mn}^{TM} are the wave impedances for the mn-th TE and TM modes [14]. Each of these is a parallel combination of the impedances in the $+z$ and $-z$ directions.

The transmission-line model for the grid is completed by adding the equivalent circuit model for the MESFET. The model for the Fujitsu FSC11X is shown in Fig. 4(b). The values for the lumped elements in the model are provided by the manufacturer and

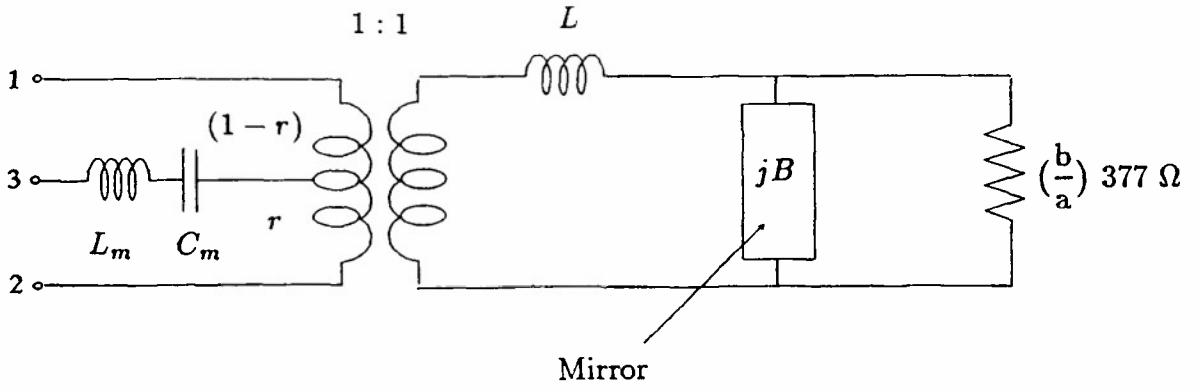

(a)

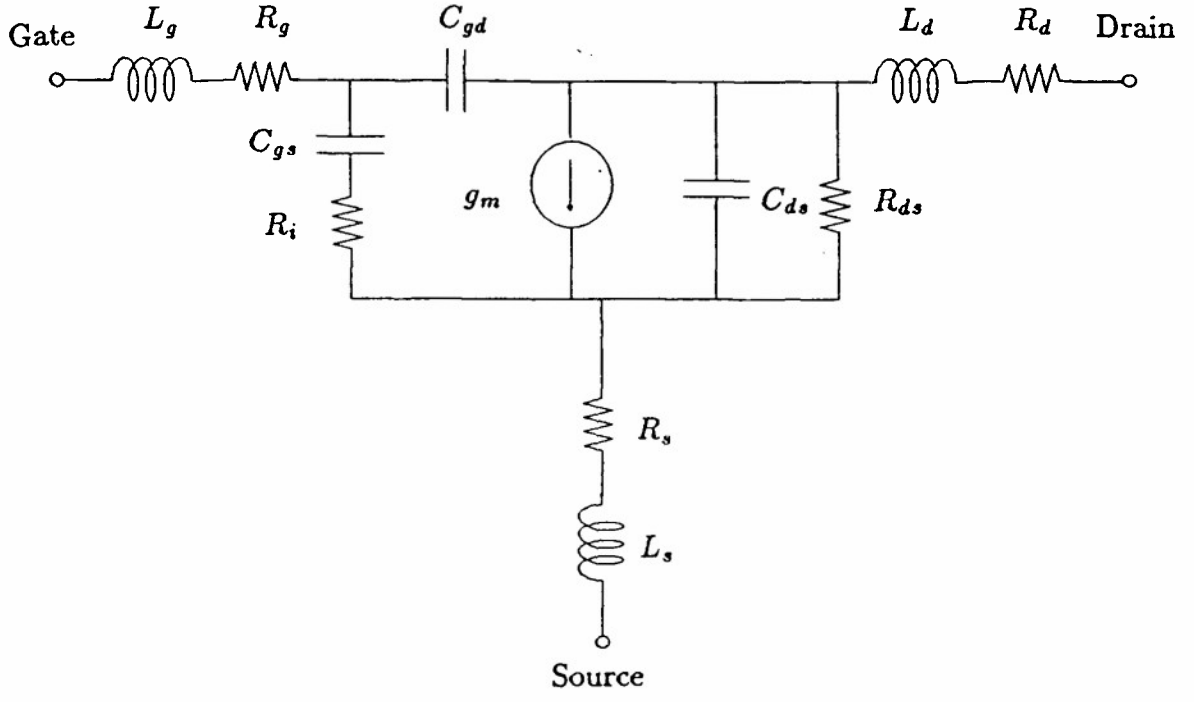

(b)

Figure 4. (a) Transmission-line model for the planar MESFET grid. The transformer turns ratio is defined as $r = c/b$. (b) Equivalent circuit for the MESFET. The values for the lumped elements are obtained from the manufacturer's data sheet.

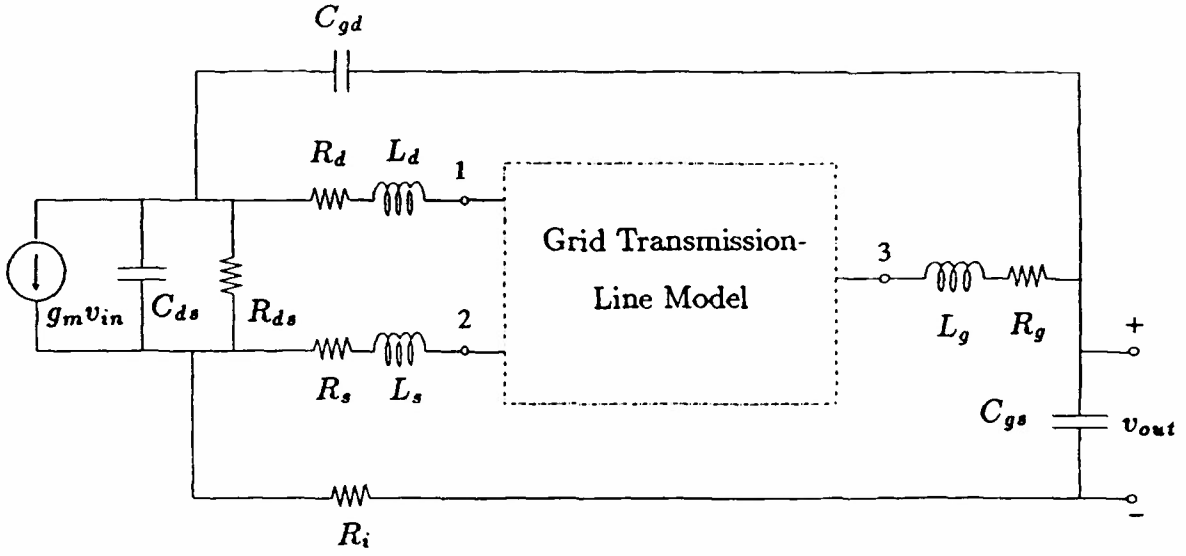

Figure 5. Circuit model used to represent the planar grid with gate feedback. The grid embedding circuit of Fig. 4(a) is denoted by the dashed box. The voltage transfer function v_{out}/v_{in} is the loop gain of the system and is used to determine the frequency of oscillation.

depend on the transistor bias point. The complete circuit representing the vertical drain-source configuration of Fig. 2(b) is shown in Fig. 5. The drain and source of the MESFET are connected to terminals 1 and 2 of the transmission-line model. Because the grid embedding network provides a feedback path between the drain and gate, we refer to the vertical drain-source configuration as a "gate feedback" grid. The transconductance current of the MESFET is controlled by the voltage appearing across the gate-source capacitor. The loop gain of the circuit can be calculated using a test voltage with the current source and finding the resulting voltage induced across the gate-source capacitor. A loop gain of magnitude greater than unity with zero phase shift indicates an oscillation.

IV. X-Band MESFET Grid

A planar-grid oscillator may be designed using the appropriate device model in the circuit of Fig. 5. The dimensions of the grid as well as the substrate thickness and dielectric constant are parameters chosen to obtain oscillation at a desired frequency. An X-band grid oscillator designed from this circuit model is shown in Fig. 6. The grid contains 16 MESFET chips (Fujitsu FSC11X) spaced 9 mm apart in both the $\hat{x}$ and $\hat{y}$-directions . These devices, which have an f_T of 19 GHz and f_{max} of 39 GHz, are typically used for low-noise C-band amplifiers. The lead widths w and w_s are 1 mm and the substrate is 2.5 mm thick Roger's Duroid with $\epsilon_r = 2.2$. To preserve the symmetries assumed in the grid model, the vertical leads are extended a quarter wavelength above and below the array. This produces a low impedance where the unit

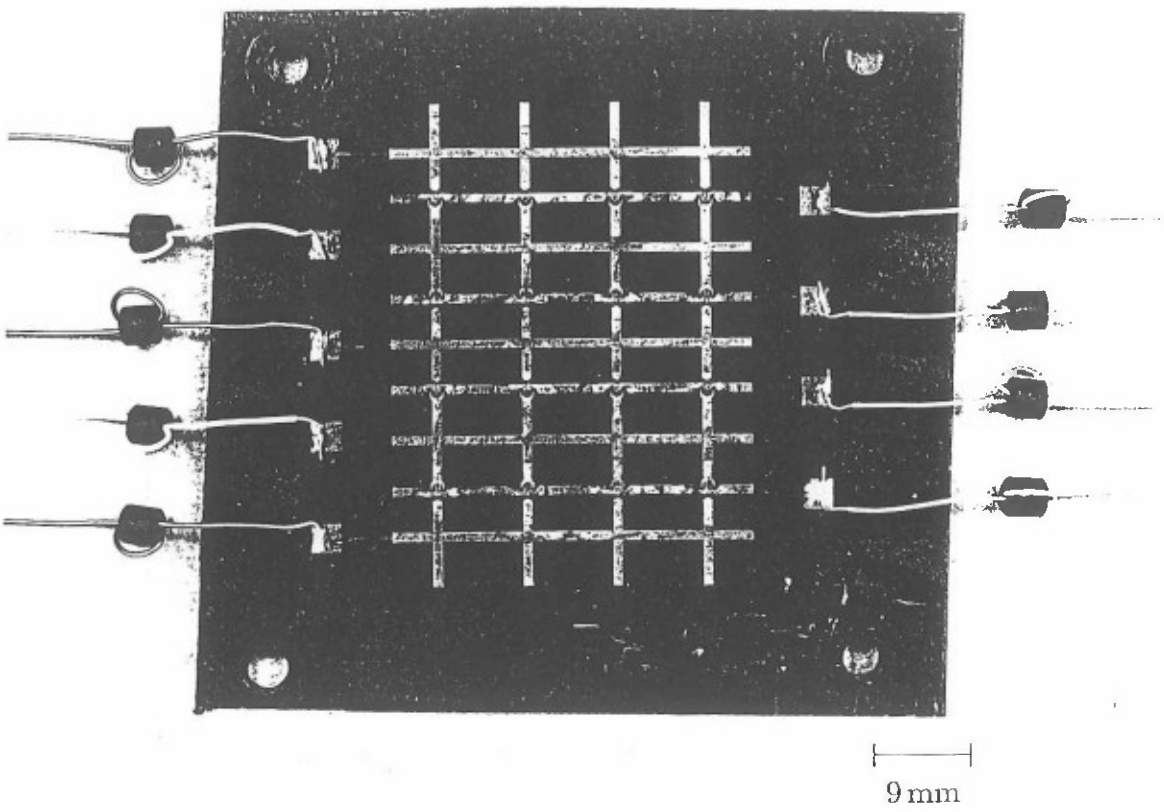

Figure 6. Photograph of the X-band grid oscillator. The substrate is 2.5 mm thick Roger's Duroid with $\epsilon_r = 2.2$. The grid is placed between a mirror and dielectric slab which from the Fabry-Perot cavity. Ferrite beads are placed on the bias lines to suppress low-frequency oscillations.

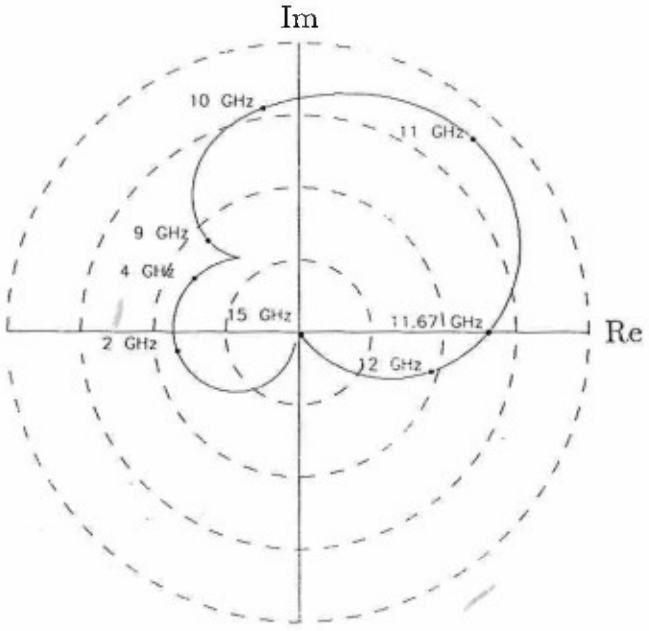

Figure 7. Calculated loop gain of the X-band MESFET grid as frequency is swept from DC to 15 GHz. The locus crosses the zero-phase point at 11.67 GHz indicating an oscillation at that frequency.

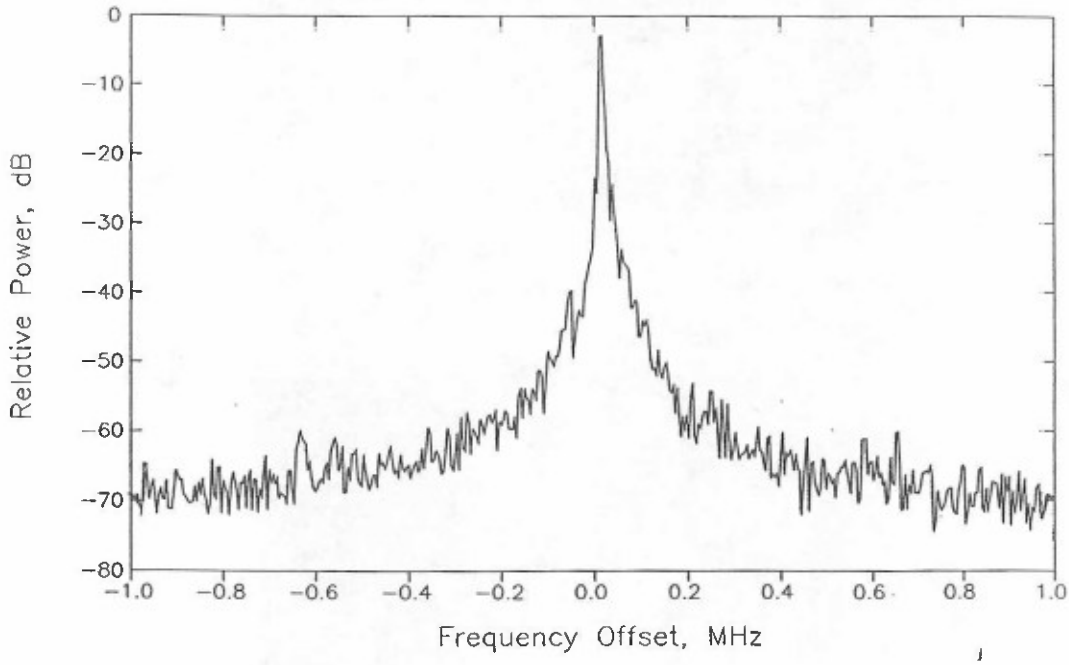

Figure 8. Spectrum of the X-band MESFET grid. The center frequency is 11.58 GHz.

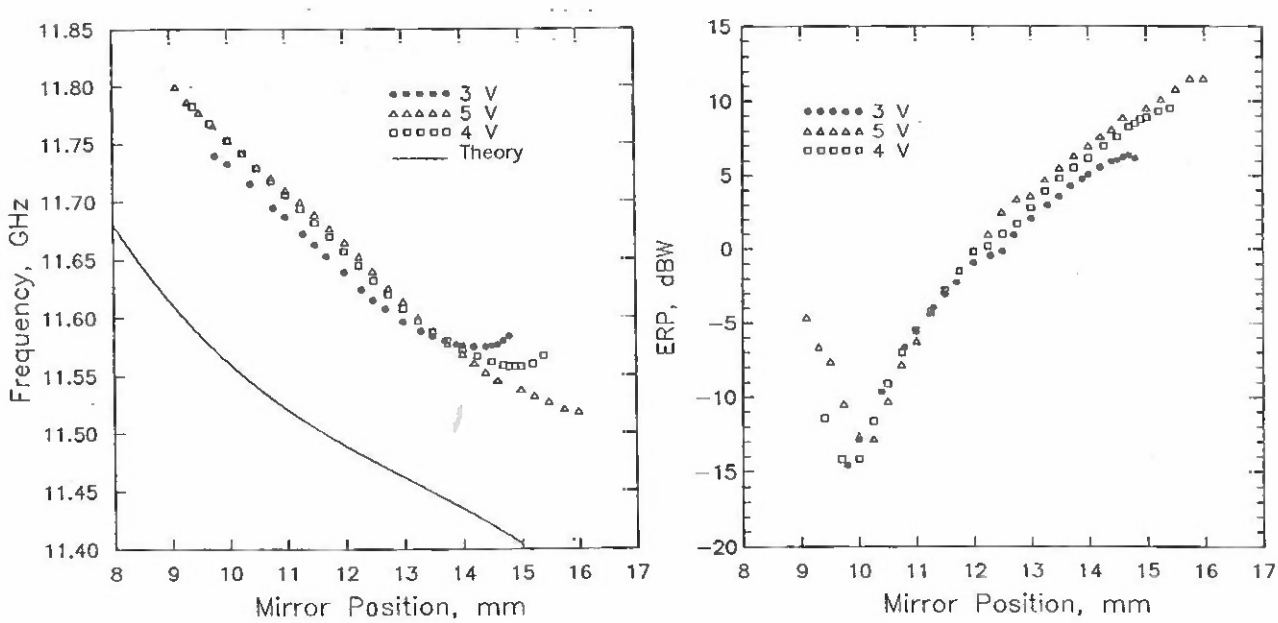

(a) (b)

Figure 9. (a) Oscillation frequency and (b) Power tuning of the grid as a function of mirror position for various drain biases. For these measurements a dielectric slab was placed 2 cm in front of the grid and the gate was biased at −1.4 V.

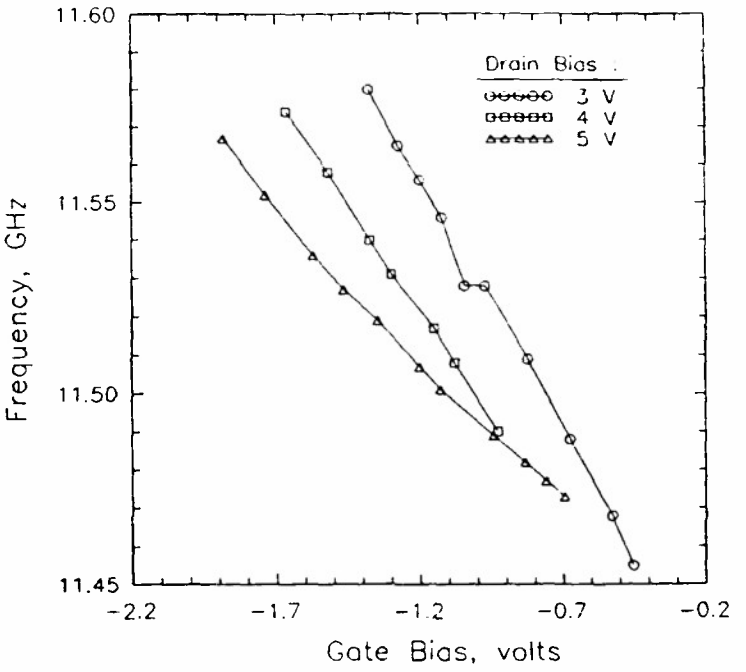

Figure 10. Measured frequency tuning with gate bias voltage. The mirror was positioned 14 mm behind the grid with the dielectric slab 2 cm in front.

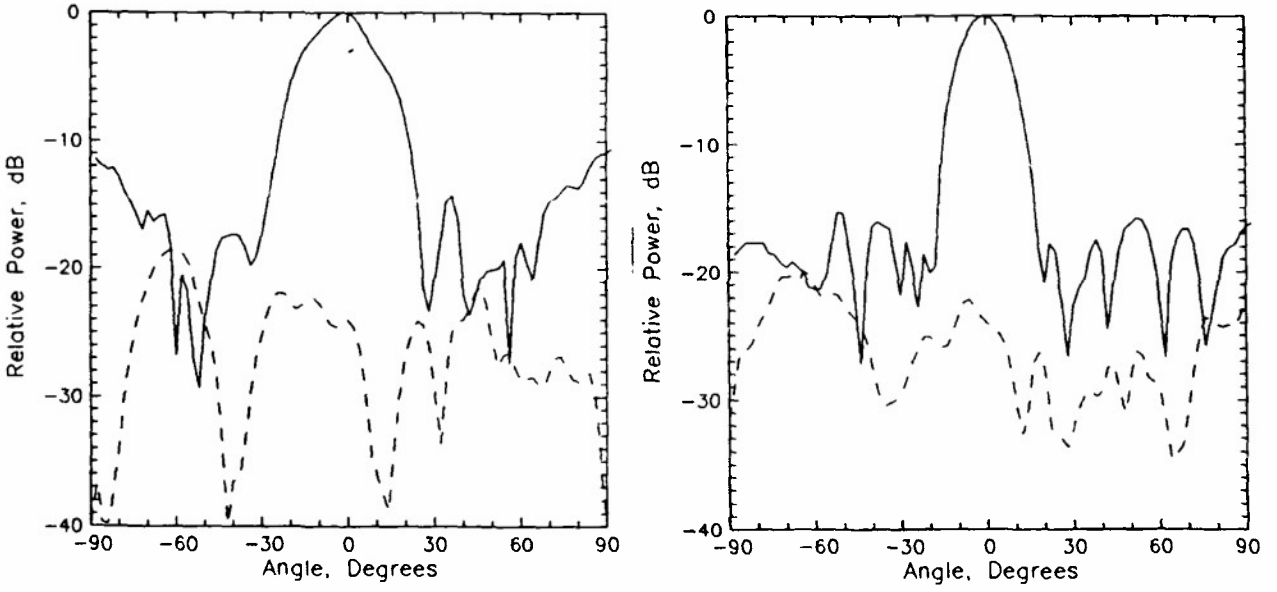

Figure 11. Measured far-field radiation patterns for the X-band grid in the H-plane (a) and E-plane (b). The cross-polarized patterns are shown with the dashed lines.

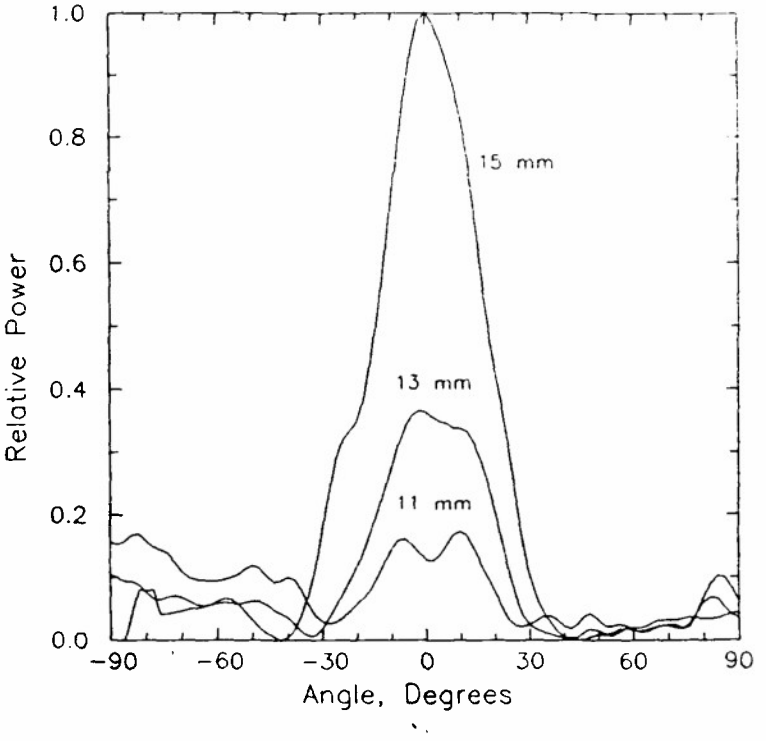

Figure 12. Far-field H-plane pattern of the X-band grid as a function of mirror position. As the mirror is moved towards the grid the directivity and radiated power decrease.

cell is assumed to have an electric wall. Bond wires are used to bring the DC bias in to the horizontal leads. The inductance of these bond wires creates a high impedance on either side of the grid where a magnetic wall is needed to maintain symmetry. From the above dimensions, the radiating lead inductance, L, is calculated to be 3.4 nH. L_m and C_m are 0.94 nH and 304 fF, respectively.

A polar plot of the loop gain v_{out}/v_{in} for the grid is shown in Fig. 7. The loop gain has a magnitude of 2.7 and zero phase at a frequency of 11.67 GHz. Fig. 8 shows the spectrum measured in the far-field when the grid was biased with a drain voltage of 3 V and current of 200 mA . The effective radiated power (ERP) was measured at 15 W. For this measurement, a planar mirror was placed 14 mm behind the grid and a dielectric tuning slab was placed 2 cm in front of the grid. The dielectric slab (1.25 mm thick with $\epsilon_r = 10.2$) was found to be helpful in locking the grid to a single frequency, but not necessary. The mirror and dielectric slab can be used to tune the frequency and power of the oscillation. These tuning curves are shown in Fig. 9 for three different bias points. A theoretical frequency tuning curve obtained from the equivalent circuit model is shown for comparison and is within 2% of the measured curve. Gate bias voltage can also be used to tune the frequency but has little effect on the output power (Fig. 10). The far-field radiation pattern measured with a standard-gain pyramidal horn at a distance of 160 cm gave a maximum directivity of 16.5 dB (Fig. 11). The antenna pattern was also a strong function of mirror position as shown

in Fig. 12. Maximum power radiated from the grid was measured to be 335 mW, or 20 mW per device. This corresponds to peak directivity and gave a DC-to-RF conversion efficiency of 20%.

V. Ku-Band MESFET Grid

An advantage of the planar MESFET grid configuration is the ease with which it can be scaled for higher-frequency operation. Simulations with the equivalent circuit model indicate that oscillations near the f_T of the transistor are obtainable. The possibility of realizing an oscillator near 100 GHz with an appropriately designed grid of psuedomorphic HEMT's is quite attractive. To explore the feasibility of scaling grids to higher frequencies, the X-band grid oscillator previously discussed was scaled for operation in the Ku-band. The Ku-band design employed the same devices (FSC11X MESFET's) as the X-band oscillator. A 36-element grid was fabricated on a Duroid substrate (2.5 mm thick and $\epsilon_r \approx 2.2$) with a device spacing of 5 mm. The lead width was scaled to 0.5 mm and extended a quarter wavelength above the top row and below the bottom row of the grid.

Simulations performed with the equivalent circuit model indicated that the grid will oscillate at 17 GHz . Single frequency operation of the Ku-band grid was verified with a spectrum analyzer. As before, the power and frequency could be tuned with the backshort (Fig. 13). The grid produced an effective radiated power of 3.3 W which corresponds to a total radiated power of 235 mW . This is equivalent to 6.5 mW per

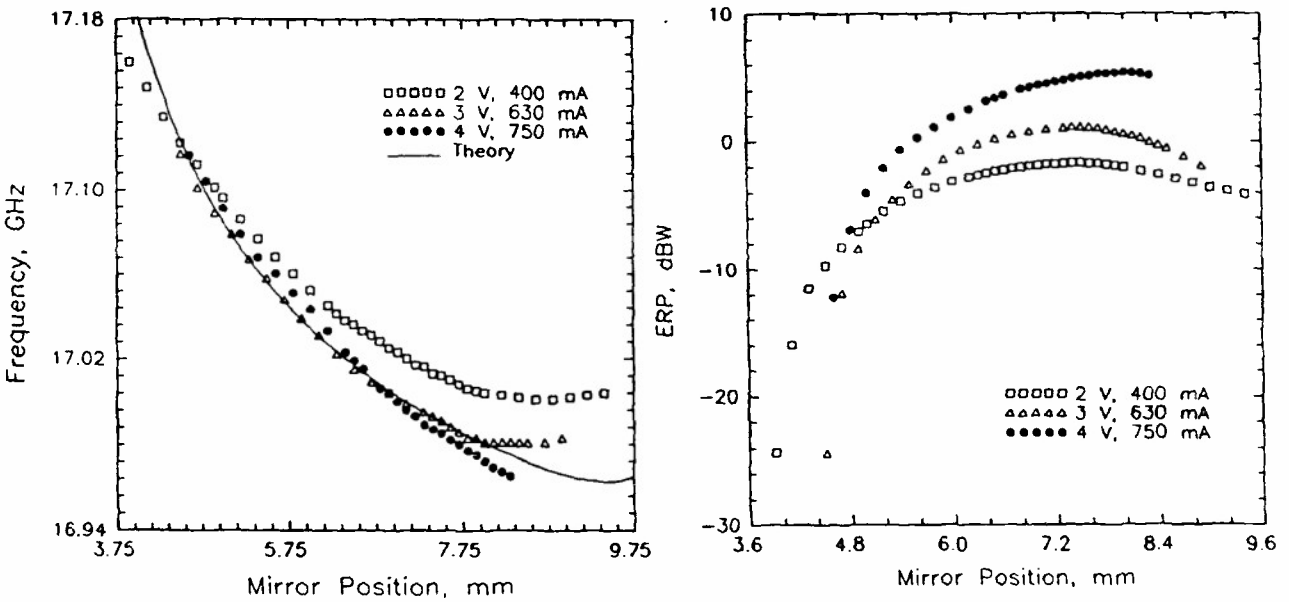

Figure 13. Frequency (a) and power (b) tuning curves of the Ku-band MESFET grid for three different bias points. The measurements were taken without the front dielectric slab.

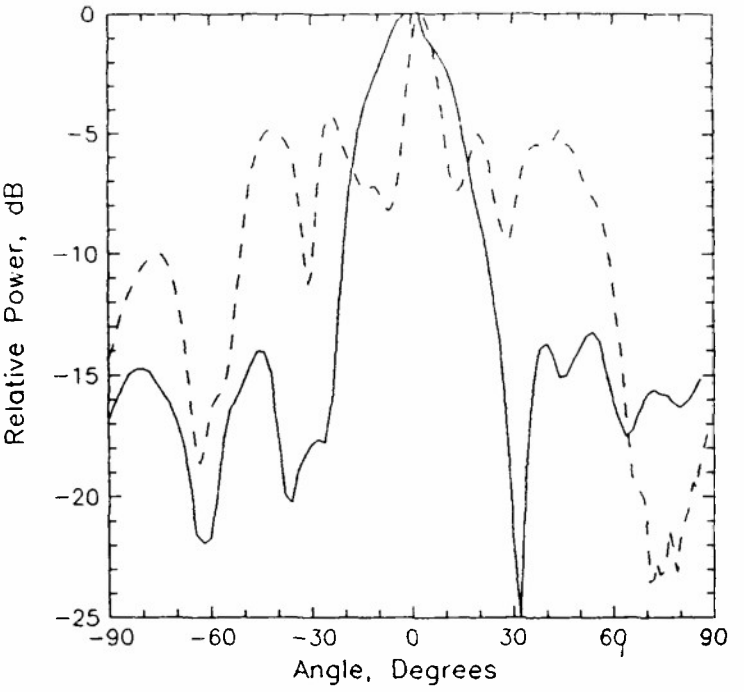

Figure 14. Measured far-field patterns in the H-plane (—) and E-plane (- - -) for the Ku-band grid oscillator.

device and gives a DC-to-RF conversion efficiency of 7%. The observed reduction in output power of the devices is expected due to the higher operating frequncy. Typically, the power available from solid-state devices decreases with the inverse square of the frequency [15]. The measured far-field antenna patterns are shown in Fig. 14. The directivity of the grid was measured to be 11.5 dB.

VI. Conclusions

A method for quasi-optical power combining with transistors has been described. The approach involves a planar periodic grid into which devices are embedded. A Fabry-Perot cavity is used to lock the devices to a single frequency which is determined by the resonator and the symmetry of the grid. The planar configuration is advantageous because it is simple and suitable for wafer-scale integration. A monolithically fabricated grid may potentially contain thousands of millimeter-wave devices for large-scale power combining. Use of a gate-feedback structure permits the grids to be operated at higher frequencies because the gate is not coupled directly to the radiated field. A transmission-line model used to predict the performance of the grid makes the design procedure straightforward. Grid oscillators are an attractive means of producing high-power radiation from solid-state sources and may be cascaded with other quasi-optical components such as grid mixers [16] and amplifiers [17] to produce a complete heterodyne receiver system.

ACKNOWLEDGMENTS

This research was supported by the Army Research Office and the Northrop Corporation. Jonathan Hacker holds an NSERC fellowship from Canada, and Michael De Lisio holds an NSF Fellowship.

REFERENCES

[1] K.J. Sleger, R.H. Abrams, R.K. Parker, "Trends in Solid-State Microwave and Millimeter-Wave Technology," *IEEE Microwave Theory and Techniques Newsletter*, no. 127, pp. 11-14, Fall 1990.

[2] T.B. Ramachandran, "Gallium Arsenide Power Sources," *Microwave J.*, pp. 91-107, 1990 State of the Art Reference.

[3] P.M. Smith, P.C. Chao, J.M. Ballingall, A.W. Swanson, "Microwave and mm- Wave Power Amplification using Pseudomorphic HEMTs," *Microwave J.* pp. 71-85, May 1990.

[4] J.A. Higgins, "GaAs Heterojunction Bipolar Transistors : A Second Generation Microwave Power Amplifier Transistor," *Microwave J.* pp. 176-194, May 1991.

[5] Kenneth J. Russell, "Microwave Power Combining Techniques," *IEEE Trans. Microwave Theory Tech.*, MTT-27, pp. 472-478, May 1979.

[6] Kai Chang and Cheng Sun, "Millimeter-Wave Power Combining Techniques," *IEEE Trans. Microwave Theory and Tech.*, MTT-31, pp. 91-107, February 1983.

[7] James W. Mink, "Quasi-Optical Power Combining of Solid-State Millimeter-Wave Sources," *IEEE Trans. Microwave Theory Tech.*, MTT-34, pp. 273-279, February 1986.

[8] Z.B. Popović, R.M. Weikle, II, M. Kim, K.A. Potter, D.B. Rutledge, "Bar-Grid Oscillators," *IEEE Trans. Microwave Theory Tech.*, MTT-38, pp. 225-230, March 1990.

[9] M. Nakayama, M. Hieda, T. Tanaka, K. Mizuno, "Millimeter and Submillimeter Wave Quasi-Optical Oscillator with Multi-Elements," *1990 IEEE MTT-S Int. Microwave Symp. Digest.* (Dallas), pp. 1209-1212, May 1990.

[10] R.A. York, R.C. Compton, "Quasi-Optical Power Combining Using Mutually Synchronized Oscillator Arrays," *IEEE Trans. Microwave Theory Tech.* MTT- 39, pp. 1000-1009, June 1991.

[11] J. Birkeland, T. Itoh, "A 16-Element Quasi-Optical FET Oscillator Power Combining Array with External Injection Locking," *submitted to the IEEE Trans. Microwave Theory and Tech.*, June 1991.

[12] Z.B. Popović, R.M. Weikle, II, M. Kim, D.B. Rutledge, "A 100-MESFET Planar Grid Oscillator," *IEEE Trans. Microwave Theory and Tech.*, MTT-39, pp. 193-200, February 1991.

[13] R.L. Eisenhart and P.J. Khan, "Theoretical and Experimental Analysis of a Waveguide Mounting Structure, " *IEEE Trans. Microwave Theory Tech.*, MTT-19, pp. 706-719, August 1971.

[14] R.F. Harrington, *Time-Harmonic Electromagnetic Fields.* New York: McGraw-Hill, 1961, p. 152.

[15] S.M. Sze, *Physics of Semiconductor Devices, 2nd ed.* New York: John Wiley & Sons, 1981, pp. 313-345.

[16] J.B. Hacker, *et. al.,* "A 100-Element Planar Schottky Diode Grid Mixer," *submitted to IEEE Trans. Microwave Theory and Tech.*, July 1991.

[17] M. Kim, *et, al.,* "A Grid Amplifer," *Submitted to IEEE Microwave and Guided Wave Letters,* June 1991.

Submitted to the *IEEE Transactions on Microwave Theory and Techniques*, July 1991

A 100-Element Planar Schottky Diode Grid Mixer

Jonathan B. Hacker, Robert M. Weikle, II, Moonil Kim
Michael P. De Lisio, David B. Rutledge

Division of Engineering and Applied Science
California Institute of Technology
Pasadena, CA 91125

Abstract—**In this work we present a Schottky diode grid mixer suitable for mixing or detecting quasi-optical signals. The mixer is a planar bow-tie grid structure periodically loaded with diodes. A simple transmission line model is used to predict the reflection coefficient of the grid to a normally incident plane wave. The grid mixer power handling and dynamic range scales as the number of devices in the grid. A 10 GHz 100-element grid mixer has shown an improvement in dynamic range of 16.3 to 19.8 dB over an equivalent single-diode mixer. The conversion loss and noise figure of the grid are equal to that of a conventional mixer. The quasi-optical coupling of the input signals makes the grid mixer suitable for millimeter-wave applications by eliminating waveguide sidewall losses and machining difficulties. The planar property of the grid potentially allows thousands of devices to be integrated monolithically.**

I. Introduction

Power-combining schemes involving solid-state devices quasi-optically coupled in free space have recently been employed to develop high-power microwave oscillators and amplifiers with directive beams [1–3]. These grid components lead the way to high-power solid-state millimeter-wave sources. However, oscillators and amplifiers are only two of many electronic components that are amenable to packaging in the grid configuration. A grid loaded with diodes produces a nonlinear device suitable for mixing or detecting quasi-optical signals with improved dynamic range compared to conventional single-diode mixers. This is particularly important for superconducting tunnel-junction (SIS) receivers where dynamic range is limited. Millimeter-wave high dynamic range front-ends are also the subject of a U.S. Navy initiative addressing current needs in its microwave electronics operational capability [4]. It should be possible to manufacture the grid mixer presented here as a planar monolithic circuit allowing a large number of diodes to be combined on a single wafer. This approach should give significant improvements in power-handling and dynamic range for mixers operating at millimeter-wave frequencies.

The planar grid mixer is shown in Fig. 1. The devices are Hewlett-Packard low-barrier Schottky beam-lead diodes (HSCH-5332), suitable for mixers and detectors operating through the Ku-band. The diodes are placed in a bow-tie shaped unit cell. The grid is fabricated on a 3.2 mm thick Duroid substrate with $\epsilon_r = 10.2$. The grid is 30 mm wide and the grid period is 3 mm. There is a flat metal mirror behind the grid to act as a reactive tuning element. The grid mixer reflection coefficient was optimized for incident signals near 10 GHz by adjusting the dimensions of the unit cell bow-tie pattern and the substrate thickness. Diodes in each column are connected in series. The IF voltages add along each column and are collected at the diode terminals forming the top and bottom edges of the grid. A DC bias is also applied at the grid edges. The symmetry of the grid cancels any RF currents along the horizontal rows.

II. Equivalent Circuit

In an infinite grid with a uniform plane wave normally incident upon the grid surface, symmetry allows us to represent the grid as an equivalent waveguide unit cell. This waveguide has magnetic walls on the sides and electric walls on the top and bottom, as shown in Fig. 2. The walls extend in the $+z$ and $-z$ directions, with the diodes in the $z = 0$ plane. In effect, this reduces the problem of analyzing the grid to that of analyzing an equivalent waveguide with electric and magnetic walls. The impedance

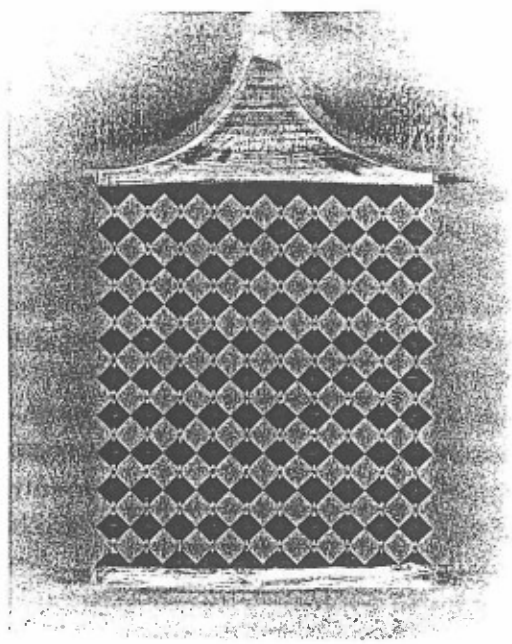

Figure 1. The 100-Element planar Schottky diode grid mixer. The incident RF and LO electric fields are polarized vertically. The IF signal is taken off the top and bottom edges of the grid. The IF impedance of the square grid is equal to the IF impedance of a single diode. The diodes are bonded to the grid with conductive epoxy.

presentcd to the terminals of a diode in the grid can be found by following a procedure similar to the EMF analysis in thc paper by Eisenhart and Kahn [5]. This approach is justified by the fact that the grid period is only $\lambda/10$. Thc calculations are described in detail by Weikle [6], and it is unnecessary to repeat them here. As a check on the EMF analysis, the grid was also modelled using the Hewlett-Packard High-Frequency Structure Simulator [7]. The HFSS is a threc-dimensional full-wave electromagnetic solver that can be used to find the fields and s-parameters of an arbitrary three-dimensional structure. The HFSS solution was in good agreement with the EMF analysis. The advantage of using the structure simulator over the EMF method is its ability to analyze arbitrary grid shapes that are too complicated for the EMF method.

For design purposes, we would like to find the reflection coefficient of an infinite grid for a plane wave at normal incidence. The equivalent circuit for the grid mixer is shown in Fig. 3. A transmission line represents the propagating TEM mode through the substrate, and the mirror is rcpresentcd as a short-circuited stub. The bow-tie grid is modelled as a short scction of transmission line with charactcristic impedance Z_{BT} and electrical length θ_{BT}. Values for Z_{BT} and θ_{BT} are obtained directly from the EMF analysis, or by parameter fitting to the HFSS simulation.

The diode is added to the model by using the manufacturer's equivalent circuit. The entire grid is in this way reduced to a one-port equivalent circuit. Simulation of the grid is carried out by calculating the reflection coefficient the grid presents to a

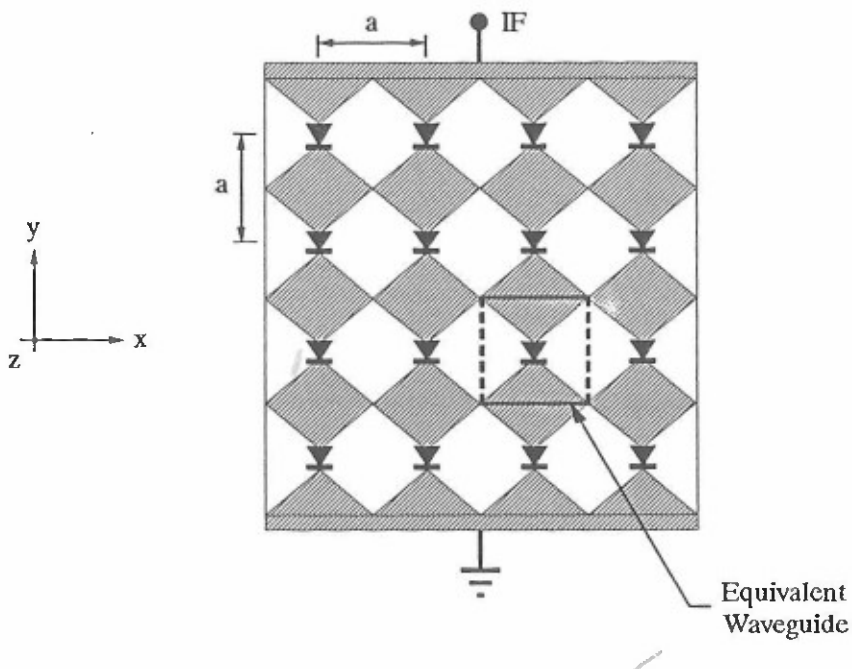

Figure 2. Layout of the Schottky diode grid mixer. Boundary conditions are imposed by the grid symmetry. The solid lines are electric walls ($E_{tangential} = 0$) and the dashed lines are magnetic walls ($H_{tangential} = 0$). In our grid, $a = 3\,\mathrm{mm}$.

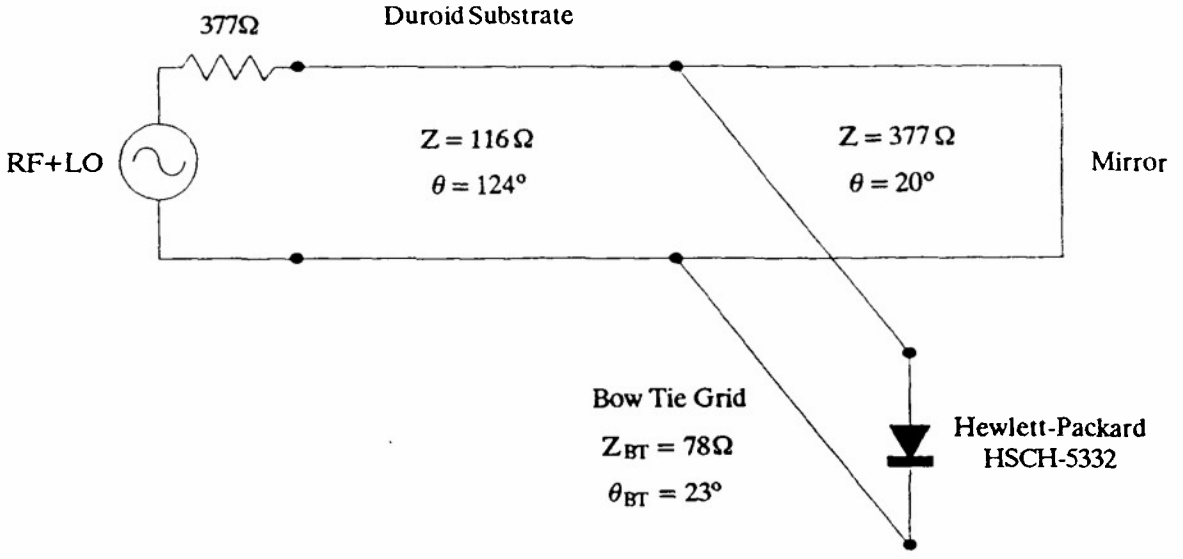

Figure 3. Transmission line model for the grid mixer. The diode is modelled using the manufacturer's equivalent circuit. The reflection coefficient of the grid was matched to free space at the design frequency of 10 GHz.

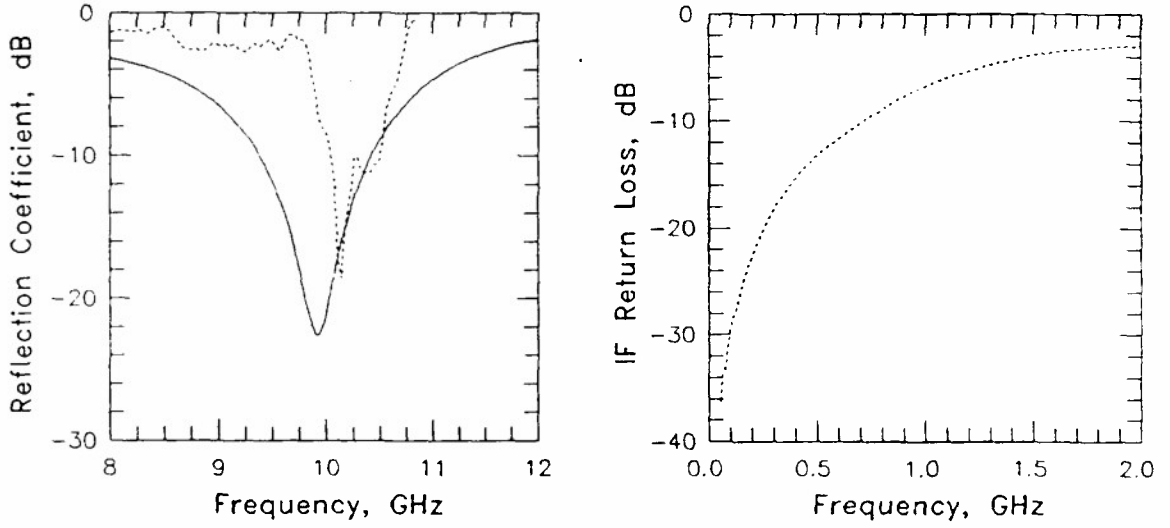

(a) (b)

Figure 4. (a) Theoretical (—) and measured (- - -) grid mixer reflection coefficient. The theoretical curve was obtained using the transmission line model developed for the grid, and the model provided by the manufacturer of the Schottky diode. (b) Measured grid mixer IF return loss with a DC bias of 4.5 mA .

normally incident plane wave in free space. The design was optimized by matching the grid to free space at the design frequency of 10 GHz.

A measurement of the grid reflection coefficient using an error-corrected quasi-optical reflectometer was found to be in reasonable agreement with theory as shown in Fig. 4(a). Fig. 4(b) shows the measured IF return loss. A small DC bias of 4.5 mA was required to match the IF impedance to 50 Ω .

III. Conversion Loss and Noise Figure

For a square grid, the conversion loss of the grid mixer will be the same as a single-diode mixer in an equivalent embedding impedance. For the purpose of comparison, a single-diode microstrip mixer was designed and built with a diode of the same type used in the grid (Fig. 5). This allows us to compare the performance of the grid to that of an equivalent single-diode mixer. The microstrip mixer employs transmission line matching circuits for the RF/LO and IF sections of the mixer [8]. The RF and LO signals were combined externally using a hybrid coupler to simplify the design. A DC bias was applied to the mixer diode through a bias-tee connected to the IF port.

Fig. 6(a) shows the measured conversion loss of the grid mixer as a function of local oscillator power per diode for a combined 10.225 GHz LO signal and a 10.439 GHz RF signal normally incident upon the grid. Fig. 6(a) also shows the measured conversion loss of the equivalent single-diode microstrip mixer. The results verify that the grid mixer conversion loss is nearly equal to the single-diode mixer. The difference can be attributed to the slightly unequal impedances presented to the diodes for the two mixer designs. A grid conversion loss of 7.9 dB was measured for a local oscillator power of −4 dBm per diode.

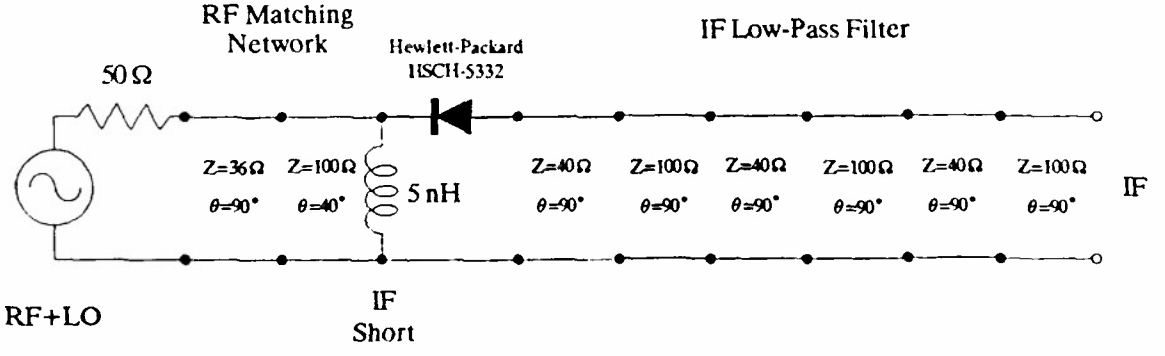

Figure 5. Schematic of the microstrip mixer used for comparison with the grid mixer. The IF low-pass filter provides a short at the RF/LO frequency. The lumped inductor shorts the RF/LO port at the IF frequency. The RF and LO signals are combined externally with a hybrid coupler. A DC bias was applied to the diode through a bias-tee connected to the IF port.

The frequency response of the grid conversion loss is shown in Fig. 6(b) for a local oscillator power of –20 dBm per diode. Again, the performance of the equivalent single-diode mixer is included for comparison. The grid is band-limited by the reactive mirror tuning element. A more sophisticated design could exploit the broadband nature of the bow-tie grid by eliminating the mirror from the system. This would permit very broad bandwidths to be achieved.

The noise power of a square grid mixer is the same as the noise power of a single-diode mixer because the individual noise powers from each diode are uncorrelated. Consequently, the noise figure of the grid mixer will be the same as an equivalent single-diode mixer. In order to measure the noise figure of the grid, a Hewlett-Packard 8970 Noise Figure Meter was modified to allow quasi-optical noise figure measurements (Fig. 7). The grid was placed in an anechoic chamber to shield the measurement system from external disturbances. Fig. 8 shows the measured noise figure of the grid for a local oscillator power of –20 dBm per diode. Again, the performance of the equivalent single-diode mixer is included for comparison. The results verify that the grid mixer noise figure and the single-diode mixer noise figure are nearly equal. The difference in noise figure can again be attributed to the slightly unequal impedances presented to the diodes for the two mixer designs.

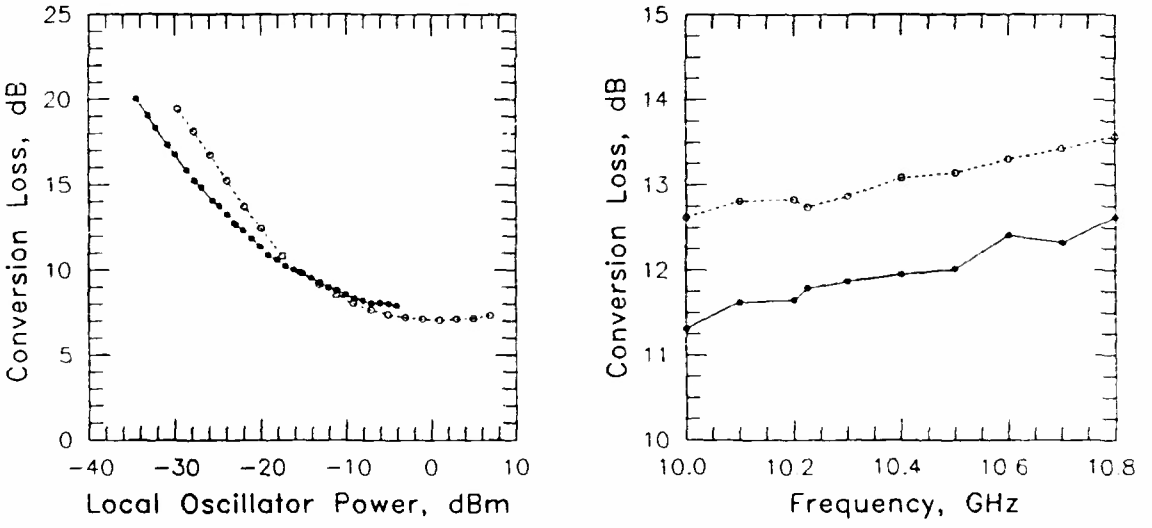

Figure 6. (a) Measured grid mixer conversion loss (—) and equivalent single-diode mixer conversion loss (- - -) as a function of LO power per diode for an LO frequency of 10.225 GHz and an IF frequency of 214 Mhz. The conversion loss of the grid mixer is comparable to the single-diode mixer. (b) Measured grid mixer conversion loss (—) and equivalent single-diode mixer conversion loss (- - -) as a function of frequency for a local oscillator power of –20 dBm per diode. The bandwidth of the grid mixer is primarily limited by the reactive tuning mirror.

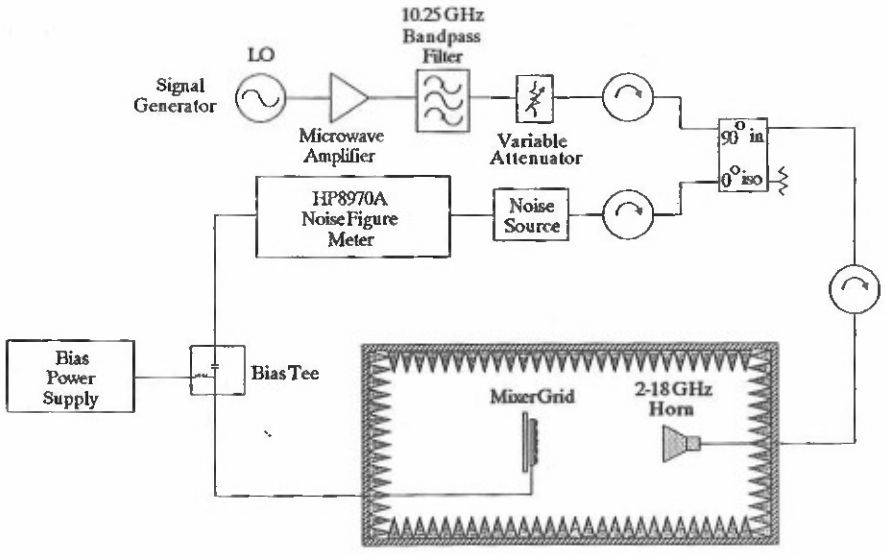

Figure 7. Quasi-optical Noise Figure meter. A high temperature noise source is used to overcome the large system path-loss. The microwave amplifier used was an HP 8349B solid-state amplifier for LO powers below –20 dBm per diode, and a 10 Watt travelling wave tube amplifier for LO powers above –20 dBm per diode.

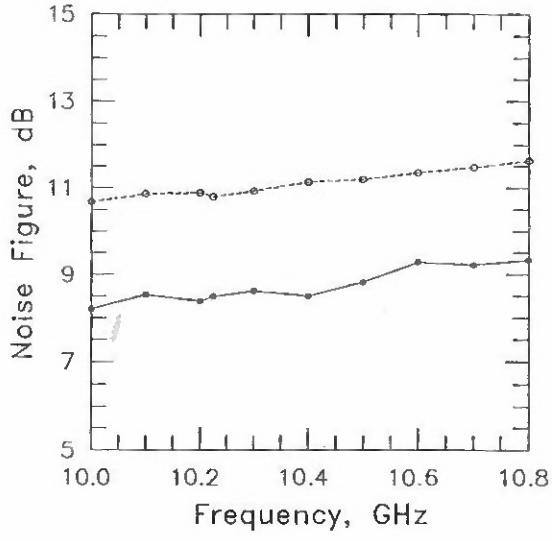

Figure 8. Measured grid mixer noise figure (—) and equivalent single-diode mixer noise figure (- - -) as a function of frequency for a local oscillator power of –20 dBm per diode. The noise figure of the grid mixer is comparable to that of a single-diode mixer. Excess noise from the TWT amplifier prevented swept frequency noise figure measurements for LO powers above –20 dBm per diode.

IV. Power Handling and Dynamic Range

An important property of the grid mixer is its ability to increase dynamic range without compromising sensitivity. Since the RF power is spread among all the devices, the saturation power of the grid is increased by a factor of the number of devices. However, the noise figure of the grid remains equal to that of a single-diode mixer. Consequently, the dynamic range is increased by a factor of the number of devices in the grid as well. Of course, the required local oscillator power is also raised by the same amount. Unlike conventional mixers, though, the power handling of the grid can be increased without bound by increasing the number of diodes in the grid. At the same time, the conversion loss and noise figure of the grid can be independently optimized by adjusting the local oscillator power per diode. This decoupling of sensitivity and power handling makes the grid mixer particularly attractive for SIS mixer designs where power handling of the nonlinear element is fundamentally limited.

In order to measure the improvement in power handling of the grid, the linearity of the grid mixer was measured and compared to the single-diode mixer. The linearity of the mixer was characterized by computing the third-order intercept point of the mixer for two equal-power RF input tones separated by 10 MHz. For the same local oscillator power per diode, the grid mixer third-order intercept point should be 100 times larger

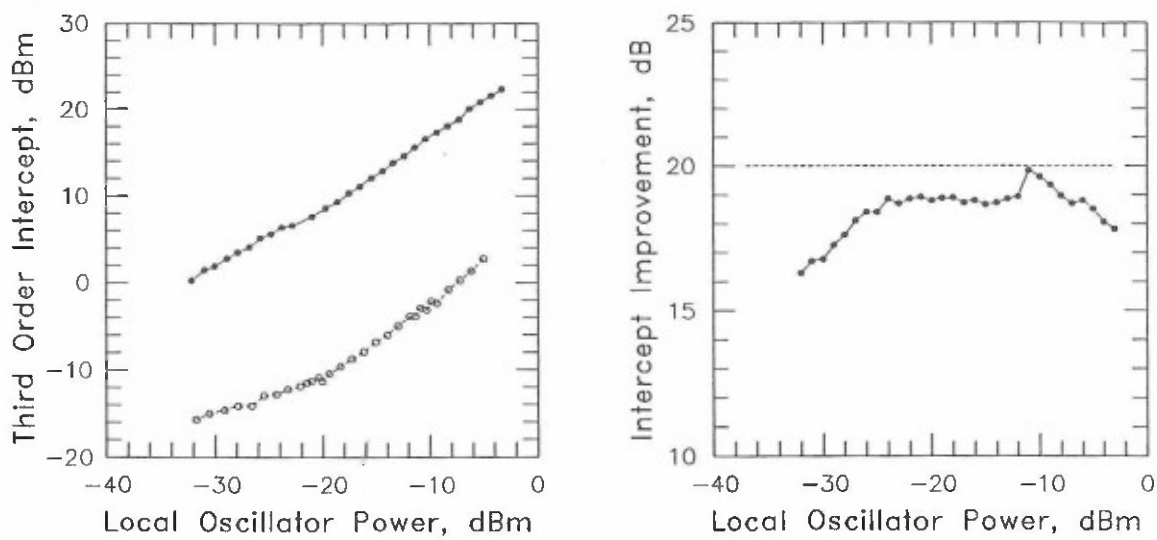

Figure 9. (a) Measured grid mixer third-order intercept point (—) and equivalent single-diode mixer third-order intercept point (- - -) as a function of local oscillator power per diode. Two RF tones at 10.434 GHz and 10.444 GHz were used to measure the intermodulation products. (b) Measured improvement in third-order intercept point for the grid mixer over the single-diode mixer (—) as a function of local oscillator power per diode. Theory (- - -) predicts a 20 dB improvement for a 100-element grid.

than that of the single-diode mixer, a factor equal to the number of diodes in the grid. Fig. 9(a) shows the measured third-order intercept point for both the grid mixer and the single-diode mixer. Fig. 9(b) shows the difference in third-order intercept point for the two mixers. Improvements of 16.3 to 19.8 dB were measured over a 30 dB range of local oscillator powers. This compares favorably with the expected improvement of 20 dB predicted from theory for a 100-element grid.

V. Conclusions

In this paper we have presented a planar grid of 100 Schottky diodes suitable for use as a quasi-optically coupled mixer. We have developed a simple transmission line model for predicting the reflection coefficient of the grid to a normally incident plane wave. We have experimentally verified that the conversion loss and noise figure of the grid mixer are comparable to a conventional single-diode mixer. We have also verified that the power handling, and hence dynamic range, of the grid mixer increases in proportion to the number of diodes in the grid. It should be possible to make a monolithic grid mixer for operation at millimeter-wave frequencies. The mixer grid is attractive for millimeter-wave applications because of its low-loss quasi-optical coupling, and because its dynamic range can be increased by a factor of the number of devices in the grid. This is important for SIS receivers where dynamic range is fundamentally limited.

Acknowledgments

This research was supported by the Army Research Office and the Northrop Corporation. Jonathan Hacker holds an NSERC fellowship from Canada, and Michael De Lisio holds an NSF Fellowship.

References

[1] Z.B. Popović, M. Kim, D.B. Rutledge,"Grid Oscillators," *International Journal of Infrared and Millimeter-Waves*, vol.9, no.7, pp. 647–654, July 1988.

[2] Z.B. Popović, R.M. Weikle, M. Kim, D.B. Rutledge,"A 100-MESFET Planar Grid Oscillator," *IEEE Trans. on Microwave Theory and Techniques*, vol.39, no.2, pp. 193–200, February 1991.

[3] M. Kim, *et al.*,"A Grid Amplifier," submitted to *IEEE Microwave and Guided Wave Letters*, May 1991.

[4] K.J. Sleger, R.H. Abrams, Jr., R.K. Parker,"Trends in Solid-State Microwave and Millimeter-Wave Technology," *IEEE Microwave Theory and Techniques Newsletter*, no.127, pp. 11–15, Fall 1990.

[5] R.L. Eisenhart and P.J. Kahn,"Theoretical and experimental analysis of a waveguide mounting structure," *IEEE Trans. Microwave Theory Tech.*, vol. MTT-19, pp. 1–87, 1983.

[6] R.M. Weikle II,"Quasi-Optical Planar Grids for Microwave and Millimeter-wave Power-Combining," Ph.D. Thesis, California Institute of Technology, Pasadena CA, 1991.

[7] "HP 85180A High-Frequency Structure Simulator," Hewlett-Packard Company, Networks Measurements Division, 1400 Fountaingrove Parkway, Santa Rosa, CA 95403, U.S.A.

[8] Stephen A. Maas, *Microwave Mixers*. Dedham MA: Artech House, 1986, pp. 181–211.

A Grid Amplifier

Moonil Kim, James J. Rosenberg, R. Peter Smith, Robert M. Weikle, II, Jonathan B. Hacker, Michael P. DeLisio, and David B. Rutledge

Abstract—**The first demonstration of a grid amplifier is reported. A 50-MESFET grid has shown a gain of 11 dB at 3.3 GHz. The grid isolates the input from the output by using vertical polarization for the input beam and horizontal polarization for the transmitted output beam. The grid unit cell is a two-MESFET differential amplifier. A simple calibration procedure allows the gain to be calculated from a relative power measurement. This grid is a hybrid circuit, but the structure is suitable for fabrication as a monolithic wafer-scale integrated circuit, particularly at millimeter wavelengths.**

I. Introduction

PERIODIC grids loaded with active devices offer the possibility of greatly increasing the power and dynamic range of solid-state components by quasi-optical power combining. A variety of active grids have been demonstrated, including phase shifters [1], multipliers [2], oscillators [3], and mixers [4]. In all these grids, circuit power scales with total area, but circuit impedances are determined by the unit cell. This allows a designer to optimize for efficiency and noise performance independently from power. Another attractive feature of the grids is that they can be made as monolithic wafer-scale integrated circuits [1], [2]. These devices could serve as building blocks for radar, communications, and imaging systems. Until now, however, the critical component has been missing—the amplifier.

II. Approach

Fig. 1 shows the approach. Vertically polarized power is incident from the left, and passes through a polarizer. The grid amplifies the beam and radiates it as horizontally polarized power, which passes through an output polarizer to the right. The polarizers are thin circuit boards with etched copper strips. These polarizers provide isolation between the input and the output. In addition, they enable independent tuning of the input and output circuits.

Fig. 2 is a diagram of our unit cell. The vertical leads pick up the incident radiation. These leads are attached to the gates of two MESFET's. These two transistors have their sources connected together, so that the pair acts as a differential amplifier. The amplified signal radiates from the horizontal drain leads. There are 25 transistor pairs in a 5-by-5 grid. The transistors are FSC10LG packaged MESFET's manufactured by Fujitsu. The substrate is a 2.54-mm thick Duroid board ($\epsilon_r = 10.5$) manufactured by the Rogers Corporation. A second Duroid board with the copper removed was placed behind the amplifier to help tune the circuit.

The bias lines are copper strips etched on the back of the substrate, parallel to the output electric field. Holes were punched in the substrate so that connections could be made to the front. The drain-bias connections are metal pins at the cell boundaries, and the gate-bias connections are 1-kΩ carbon resistors. The source-bias connections are made with 120-Ω resistors to suppress common-mode oscillations. The resistors do not affect differential gain, which determines the overall grid gain.

We can draw a simple equivalent circuit for the unit cell (Fig. 3). Free space is represented as a transmission line with a characteristic impedance of 377Ω. The Duroid substrate

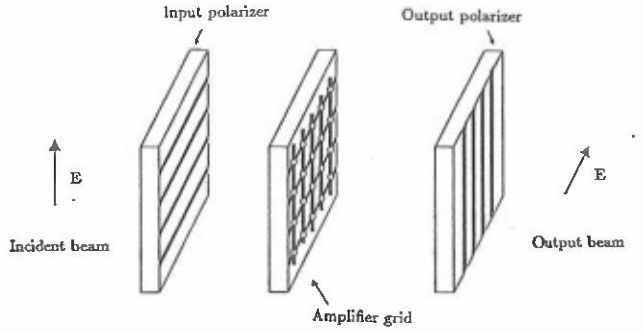

Fig. 1. Grid amplifier.

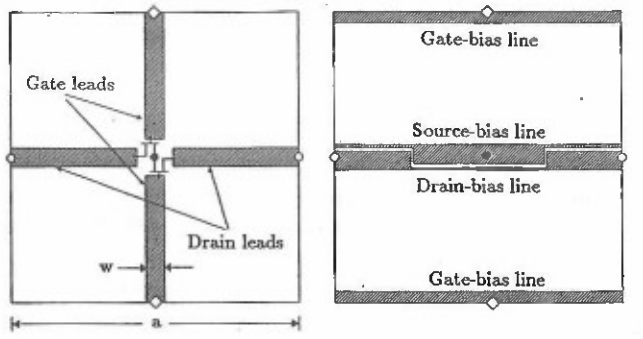

Fig. 2. Unit cell of a grid amplifier. (a) Front view. (b) Back view. Symbols indicate different connections between the front and the back of the grid amplifier. ●: 120-Ω source-bias resistor, ◇: 1-kΩ gate-bias resistor, ○: drain-bias pin.

Manuscript received May 13, 1991; revised June 21, 1991. The work done at Caltech was supported by the Army Research Office, the Northrop Corporation, and a fellowship from the Rockwell International Trust. The work done at the Jet Propulsion Laboratory was supported by the Innovative Science and Technology Office at SDIO. J. Hacker holds an NSERC Fellowship from Canada, and M. DeLisio holds an NSF Fellowship.

M. Kim, R. M. Weikle, II, J. B. Hacker, M. P. DeLisio, and D. B. Rutledge are with the Division of Engineering and Applied Science, California Institute of Technology, Pasadena, CA 91125.

J. J. Rosenberg and R. P. Smith are with the Center for Space Microelectronic Technology, Jet Propulsion Laboratory, 4800 Oak Grove Drive, Pasadena, CA 91109.

IEEE Log Number 9103567.

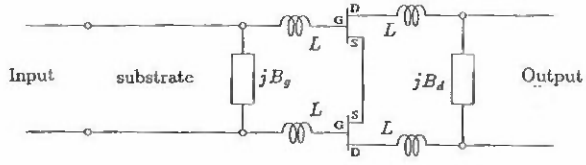

Fig. 3. Transmission-line model for the unit cell.

appears as a section of line with an impedance of 116Ω. The gate and drain leads are taken into account by an inductance that can be calculated from a quasi-static formula [5].

$$L = \left(\frac{\mu_0 a}{4\pi}\right) \ln\left[\csc\left(\frac{\pi w}{2a}\right)\right], \tag{1}$$

where a is the period, and w is the lead width. For our grid, $a = 16$ mm and $w = 2$ mm, so that $L = 2.6$ nH. The susceptance B_g represents the output polarizer, and B_d accounts for the bias lines and the input polarizer. A circuit simulation of this model using the manufacturer's scattering parameters, but neglecting the polarizers, predicts a peak gain of 8.4 dB at 3.3 GHz, with a 3-dB bandwidth of 2.4 GHz.

III. Measurements

Fig. 4(a) shows how the gain was measured. A signal generator transmits a vertically polarized beam from a small horn. The beam is incident on the grid, amplified, and transmitted with horizontal polarization. Another horn receives the amplified beam. We define the grid amplifier gain G by the equation.

$$P_r = GP_t \left(\frac{G_t A}{4\pi r^2}\right)\left(\frac{G_r A}{4\pi r^2}\right), \tag{2}$$

where P_r is the received power and P_t is the signal generator power. G_t and G_r are the gains of the transmitting and receiving horns, A is the geometrical area of the grid, and r is the distance between the grid and each horn. The terms in parentheses are the input and output space-loss factors. The grid gain G is the ratio of the power radiated by the grid to the incident power, reduced by the losses from amplitude and phase errors across the grid. This equation has quite a few parameters, but we can eliminate some of them by making a calibration measurement with the grid removed (Fig. 4(b)). The received power P_c is then given by

$$P_c = \frac{P_t G_t G_r \lambda^2}{(4\pi)^2 (2r)^2}. \tag{3}$$

From these two equations, we can write an expression for the amplifier gain as

$$G = \frac{P_r}{P_c}\left(\frac{\lambda r}{2A}\right)^2. \tag{4}$$

This simple formula allows us to calculate the gain from a relative power measurement and three well-known parameters. In our measurements, $r = 50$ cm and $A = 64$ cm^2.

Fig. 5 is a plot of the measured amplifier gain. The largest value is 11 dB at 3.3 GHz, with a 3-dB bandwidth of 90 MHz. The tuning provided by polarizers is important; we did not see gain without them. At the same time, the polarizers may be responsible for the small bandwidth. The gate bias-line voltage was −0.25 V relative to the source bias-line, and the drain bias-line voltage was 4 V. The drain current was 6.6 mA per MESFET. For comparison, the gain was also measured with the bias turned off, and it was below −5 dB everywhere. The horns have a wide bandwidth, 2 GHz to 18 GHz, and this allowed us to monitor the received signal with a spectrum analyzer to insure that there were no spurious oscillations. As an additional check, the measurements were repeated at different power levels to make sure that the output power varied linearly with input power.

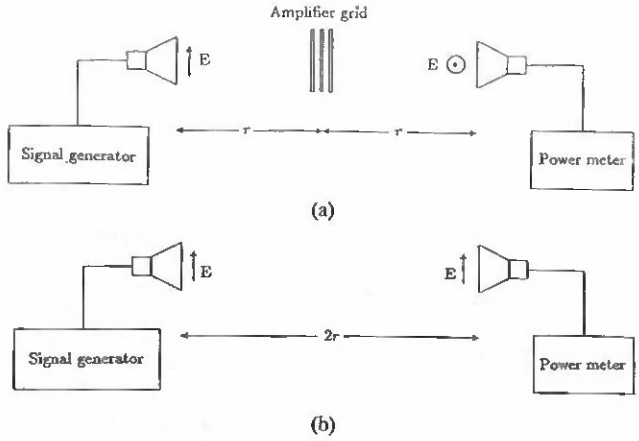

Fig. 4. (a) Measuring the amplifier gain. Gain of each horn is about 10 dB in this frequency range. (b) Calibration measurement with the grid removed and the receiving horn rotated 90° to match the transmitter polarization.

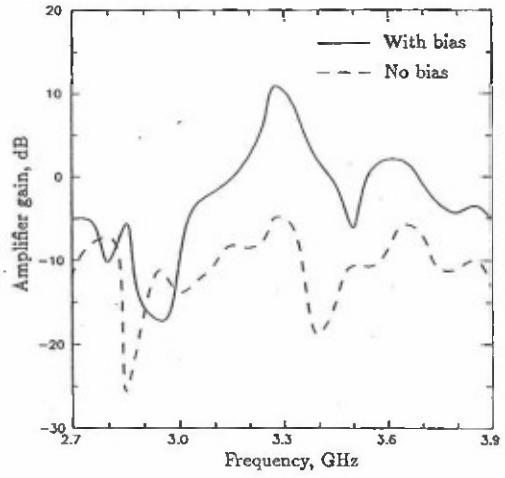

Fig. 5. Measured grid amplifier gain with bias (solid line) and without (dashed line). The total incident power was about 300 μW.

IV. Conclusion

We have demonstrated a hybrid grid amplifier with a gain of 11 dB at 3.3 GHz. Fifty MESFET's are arranged as 25 differential amplifiers that accept a vertically polarized input and transmit a horizontally polarized output. A simple calibration procedure allows the gain to be calculated from a relative power measurement. The design should be suitable

for monolithic wafer-scale integration, particularly at millimeter wavelengths.

A grid amplifier is a multimode device, and should amplify beams at different angles. For example, it should be possible to place a grid amplifier after an electronic beam-steering array. The grid would amplify both single and multiple transmitted beams, while preserving propagation angles, sidelobe levels, and monopulse nulls. The amplifier could overcome losses in the beam steerer itself. A grid amplifier could also precede a receiving beam-steering array, allowing the noise performance to be determined by the grid, rather than by losses in the beam steerer.

References

[1] W. W. Lam *et al.*, "Millimeter-wave diode-grid phase shifters," *IEEE Trans. Microwave Theory Tech.*, vol. 36, pp. 902–907, May 1988.

[2] C. F. Jou *et al.*, "Millimeter-wave diode-grid frequency doubler," *IEEE Trans. Microwave Theory Tech.*, vol. 36, pp. 1507–1514, Nov. 1988.

[3] Z. B. Popović, R. M. Weikle, M. Kim, and D. B. Rutledge, "A 100-MESFET planar grid oscillator," *IEEE Trans. Microwave Theory Tech.*, vol. 39, pp. 193–200, Jan. 1991.

[4] J. B. Hacker, R. M. Weikle, M. Kim, D. B. Rutledge, "A 100-element Schottky diode grid mixer," *IEEE AP-S Int. Symp.*, London, ON, Canada, June 1991.

[5] G. G. MacFarlane, "Quasi-stationary field theory and its application to diaphragms and junctions," *Proc. IEEE*, vol. 93, pt. 3A, pp. 1523–1527, 1946.